Cofactor NAD(P)H Regeneration Inspired by Heterogeneous Pathways

Xiaodong Wang,[1,5,*] Tony Saba,[1] Humphrey H. P. Yiu,[2] Russell F. Howe,[3] James A. Anderson,[1] and Jiafu Shi[4,*]

[1]Chemical and Materials Engineering, School of Engineering, University of Aberdeen, Aberdeen AB24 3UE, Scotland, United Kingdom

[2]Chemical Engineering, School of Engineering & Physical Sciences, Heriot-Watt University, Edinburgh EH14 4AS, Scotland, United Kingdom

[3]Department of Chemistry, University of Aberdeen, Aberdeen AB24 3UE, Scotland, United Kingdom

[4]School of Environmental Science and Engineering, Tianjin University, Tianjin 300072, China

[5]Lead Contact

*correspondence: x.wang@abdn.ac.uk

*correspondence: shijiafu@tju.edu.cn

SUMMARY

Biocatalysis can empower chemical, pharmaceutical and energy industries, where the use of enzymes facilitates low-energy, sustainable methods of producing high-value chemicals and pharmaceuticals that are otherwise impossibly troublesome or costly to obtain. One of the largest class of enzymes (oxidoreductases, ~25% of the total) capable of promoting bioreduction reactions are vital for the global pharmaceutical and chemical market due to their intrinsic enantioselectivity and specificity. Enzymatic reduction is dependent on a coenzyme/cofactor as hydride source, namely nicotinamide adenine dinucleotide, NADH or its phosphorylated form (NADPH). Given the high cost, stoichiometric usage, and physical instability of NAD(P)H, a suitable method for NAD(P)H regeneration is essential for practical application. This review summarizes the existing methods for NAD(P)H regeneration including enzymatic, chemical, homogeneous catalytic, electrochemical, photocatalytic and heterogeneous catalytic routes. Particular focus is given to recent progress in developing heterogeneous systems with potential significance in terms of process simplicity, cleanliness and energy/cost saving.

Keywords: Cofactor Regeneration; NADH; NADPH; Method; Heterogeneous Catalysis; Photocatalytic; Electrochemical; Enzymatic; Homogeneous Catalysis; Hydrogen (H_2).

INTRODUCTION

Biocatalysis has been extensively used in the chemical and pharmaceutical industries for the manufacture of products ranging from speciality[1] to commodity chemicals (*ca.* 50,000 ton/annum).[2] Enzymatic specificity and enantioselectivity are critical, notably in the pharmaceutical sector where enzymes are employed in the commercial synthesis of two thirds of chiral products[3] that are used in new drug syntheses.[1,4] For example, the drug Lipitors (atorvastatin) recorded a global sale of US$11.9 billion in 2010 alone,[1] while worldwide prescription drug sales are forecast to reach US$1,000 billion in 2020,[5] where approximately 95% of pharmaceuticals will be chiral.[6] Oxidoreductases are one of the largest class of enzymes (~25% of all enzymes) with far ranging industrial and research significance in the reduction of carbonyl groups, acids, C=C double bonds, nitro groups and C–N multiple bonds.[4,7] However, many of these enzymatic redox reactions require one or more cofactors that are consumed during reaction.[1] For instance, enzymatic reductions require a cofactor (or coenzyme) as the hydrogen source (hydride donor), notably (reduced) nicotinamide adenine dinucleotide (NADH) and its phosphorylated form (NADPH, both refer to the bioactive 1,4-NAD(P)H in this study, see **Figure 1** for their structures) where 80% of known oxidoreductases require the former and 10% require the latter.[7] In an enzymatic reduction cycle, NAD(P)H serves as a reductant which is oxidized to $NAD(P)^+$ (structure given in **Figure 1**), while the substrate is reduced to the target product using the appropriate (production) enzyme, as illustrated in "pathway A" (**Figure 2**). Given the high cost of NAD(P)H (bulk price per mol: NADH, US$3,000; NADPH, US$215,000),[8] stoichiometric supply is not economically feasible and an effective system of cofactor regeneration is required to enable practical large-scale application of enzymatic reductions. This is indeed a reason why cofactor-dependent enzymes (*e.g.*, dehydrogenases) lag behind 'simple' cofactor-

independent enzymes (*e.g.*, hydrolases and oxidases) in terms of their implementation by industry.

METHODS OF COFACTOR NAD(P)H REGENERATION

A major difference between the NAD(P)H and $NAD(P)^+$ structure is a hydride ion, *i.e.*, H^- ($H^+ + 2e^-$). Regeneration of NAD(P)H requires a (catalytic or non-catalytic) transfer of a proton and two electrons (from sacrificial hydride donors) to $NAD(P)^+$ (*i.e.*, reduction of $NAD(P)^+$). Common sacrificial hydride donors include formate, glucose, phosphite, triethanolamine (TEOA), mercaptoethanol, propanol and molecular H_2 gas, most of which are valuable chemicals but are consumed in regeneration, while some produce further waste byproducts. Typically, the activity of cofactor regeneration can be measured by turnover frequency (*TOF*, the number of moles of NAD(P)H formed per moles of active site per unit time) whereas the efficiency of an *in situ* regeneration system can be measured by turnover numbers (*TN*, the number of moles of product formed per mole of cofactor per unit time) and total turnover numbers (*TTN*, the number of moles of product formed per mole of cofactor during the course of a complete reaction). In general, *TTN*s greater than 1000 may appear to make a process economically viable.[4,9] Moreover, selectivity presents another challenge for the regeneration of NAD(P)H (**Figure 2**) as enzymatically inactive byproducts including the isomers 1,6-NAD(P)H and NAD_2 dimer may form irreversibly, leading to a permanent loss of valuable cofactor. Ultimately, the development of NAD(P)H regeneration must consider activity, selectivity, process sustainability (waste and byproduct generation) and, more importantly, the practical applications, *i.e.*, compatibility with production enzymes. It is noteworthy from the outset that there are systems which suffer from mutual deactivation between the regeneration and enzymatic processes.[10,11]

In general, methods for cofactor NAD(P)H regeneration can be sub-divided into six categories, namely enzymatic regeneration (*e.g.*, using glucose (GDH) or formate (FDH) dehydrogenases), chemical regeneration (using inorganic salts such as sodium dithionite ($Na_2S_2O_4$), sodium borohydride ($NaBH_4$) or dihydropyridine compounds, *e.g.*, 1,4-dihydropyridines), homogeneous catalytic regeneration (*e.g.*, Rh, Ru and Ir complexes), electrochemical regeneration (including both direct regeneration on the electrode and indirect regeneration using organometallic complexes as hydrogen transfer agents), photocatalytic regeneration (*e.g.*, copolymers and carbon nitride as a photocatalyst) and heterogeneous catalytic regeneration (*e.g.*, using Pt/Al_2O_3). The latter of these was recently developed by some of the authors here.[12] Cofactor regeneration has been an appealing topic with several key reviews based on discussion of the first five methods. Critical assessments to be highlighted are those by Ward and coworkers (recent trends with emphasis on approaches to overcome mutual inhibition),[10] Wu and coworkers (literature survey on the state-of-art research and crucial issues),[7] Hollman and coworkers (photocatalytic regeneration,[13] coupling with enzymatic reductions,[4] nonconventional regeneration[9]), Vincent and coworkers (H_2-driven enzymatic regeneration[14] and immobilized enzymes on carbon based materials[15]), Liu and Wang (membrane entrapment and solid attachment of cofactors),[16] Liese and coworkers (coupled with ketone reductions),[17] Hummel and coworkers (principles and examples of small-scale and industrial applications),[18] van der Donk and Zhao (developments of technologies between 2000-2003),[19] Wichmann and coworkers (lab scale regeneration[20] and regeneration in membrane reactors),[21] and Chenault and Whitesides (regeneration for use in organic synthesis).[22] In this review, discussion is directed at potentially promising systems with a "heterogeneous" nature (*i.e.*, using solid-state catalytic materials in liquid media) for clean cofactor NAD(P)H regeneration. This is of great significance because sustainable manufacturing becomes crucial for the pharmaceutical sector, where negative environmental

impact has been highlighted since the 1990s due to the low process efficiency and high waste to product ratio.[23] We first present an overview of NAD(P)H regeneration methods, then discuss in particular the approaches involving heterogeneous component(s) and finally focus on our own findings using supported metals as heterogeneous catalyst.

Enzymatic Regeneration

Cofactor regeneration using enzymes has been considered as a favorable system and has been the only one applied practically at industrial scale. One of the earliest examples demonstrating enzymatic NAD(P)H preparation from $NAD(P)^+$ was published in 1957 when ethanol and ADH were used by Rafter and Colowick.[24] Enzymatic approaches for regeneration offer excellent compatibility with the target bioconversions due to comparable reaction conditions, *i.e.,* low temperature operation in an aqueous media at a near neutral pH (5-9). Moreover, enzymatic regeneration usually associates with a high specific activity, exclusive selectivity towards the active NAD(P)H and low energy consumption. Two common strategies employed are (i) "coupled-enzyme" (**Figure 3A**) which utilizes a second enzyme (*i.e.,* regeneration enzyme) such as GDH with associated sacrificial hydride donor (*e.g.,* glucose) and (ii) "coupled-substrate" **(Figure 3B)** that one enzyme serves both reduction of substrate and cofactor regeneration. The most widely used enzymes for cofactor regeneration in commercial processes are GDH and FDH, while phosphite (PDH), alcohol (ADH), glucose 6-phosphate dehydrogenases and hydrogenases have been tested at laboratory scale.[4] **Figure 3C** depicts the reaction schemes for these cofactor regeneration systems. Among these enzymes, GDH (*e.g.,* from *Bacillus* species) shows the highest activity (up to 550 U mg^{-1}; 1 U = 1 μmol min^{-1}) and stability, and consequently has become the most widely used. FDH does have a unique feature in generating carbon dioxide (CO_2) as a

gaseous byproduct (albeit release to the environment should be minimized) for simplified product separation, but its use is hampered by its low activity (~10 U mg^{-1}).

In a "coupled-substrate" system, the single enzyme acts as both reducing (production) and oxidizing (cofactor regeneration) catalysts. One classic example is using ADH for the synthesis of the high value drug precursor (*S*)-2-bromo-2-cyclohexen-1-ol.[25] In this system, 2-propanol was chosen as the sacrificial hydride donor to form acetone, a volatile byproduct which assisted removal. This approach allows easy scale-up and simplified downstream recovery/reuse of enzyme. However, such systems typically require high concentrations of the sacrificial alcohol to drive the equilibrium towards the desired product. This in turn leads to loss of activity in the main target reaction due to competition amongst substrates and cosubstrates for the same active sites on the enzyme.

Although it is the only method industrially employed, cofactor regeneration using enzymes is far from perfect. Firstly, the generation of significant quantities of water-soluble byproducts (*e.g.*, 196 g gluconic acid per mol NADH regenerated by GDH)[4] requires costly downstream separation and causes enzyme deactivation. Additionally, base or acid may be needed to maintain the optimal pH for retaining the enzymatic action. Other disadvantages are linked to the high cost, instability of enzymes and complexity of product purification. As a result, research and development for cofactor regeneration are driven towards systems that show high stability, sustainability and enhanced downstream product separation/purification.

Chemical Regeneration

Chemical regeneration involves use of the high redox potential of salts or dihydropyridine compounds to reduce $NA(P)D^+$ to NAD(P)H, which can be considered as a non-catalytic process. Common reducing agents used include $Na_2S_2O_4$, $NaBH_4$ and 1,4-dihydropyridines. For instances, Jones *et al.*[26] in 1972 reported the possibility of utilizing $Na_2S_2O_4$ at a

preparative scale and later in 1976 reported the use of a group of reducing 1,4-dihydropyridines with different functional groups (such as $-CONH_2$, $-CO_2C_2H_5$, $-COOH$, $-CON(CH_3)_2$, *etc*.).[27] Since the corresponding *TN*s of this process are very low (*TTN* < 100) and high concentration of reductant salts can cause enzyme deactivation,[7,28] this method has interest only from a historical perspective. It is noteworthy that these methods based on non-catalytic chemical reactions (reducing potentials) have not been widely used due to intrinsic issues that include the large amount of feed required and wastes generated, whose high concentration deactivates the production enzymes.

Homogeneous Catalytic Regeneration

Cofactor regeneration using homogeneous catalysis has been reported since the 1980s using organometallic complexes as the catalysts and molecular hydrogen as the hydride source[29,30]. The most commonly employed catalysts for this purpose are complexes of transition metals such as Rh, Ru, Ir and Pt, which are known to catalyze reduction reaction. Among them, the versatile cationic pentamethylcyclopentadienyl (Cp*) rhodium bipyridine complex $[Cp^*Rh(bpy)Cl]^+$ has been most widely used due to its flexible (electro)chemical regeneration and regiospecific performance.[31] A similar approach is the combination of a Pt carbonyl cluster with the dye safranine in a two-phase system.[32] There are also examples of using these organometallic complexes supported on electrodes for electrochemical regeneration of cofactor (to be discussed later). When compared with enzymes, these organometallic complexes usually exhibit a lower catalytic activity (k_{cat} = 0.5-10 *vs.* ~100 min^{-1} for enzymes), making them less competitive when compared with their enzymatic counterpart.[10,11] Another major obstacle for large scale application of cofactor regeneration using homogeneous organometallic catalysts lies in their strong interaction with peptide components in enzymes, causing mutual deactivation.[11] However, progress made in water-

soluble organometallic catalysis has shown *TOF*s up to ~1000 h^{-1} (over Cp*Rh(5,5'-CH_2OH-bpy)Cl]$^+$)[31] and 2000 h^{-1} (over [(η^5-C_5Me_5)Rh(1,10-phenanthroline)Cl]$^+$ with demonstrated enzymatic compatibility),[33] respectively; but both were operated at 60 ℃ and still require an organic hydride donor (*i.e.*, formate). The toxicity of organometallic complexes and the necessary energy-intensive separation stages are disadvantages.

Electrochemical Regeneration

Electrochemical methods for NAD(P)H regeneration have long been acknowledged as attractive due to the low cost of electricity and the easy control of electrode potentials.[18] Regeneration could be achieved from direct, indirect or indirect enzyme-coupled recycling systems (**Figure 4**, protons supplied from the buffered solution[10]). For direct regeneration (**Figure 4A**), NAD(P)$^+$ is reduced on the electrode surface *via* a 2-step reaction mechanism. In the first step, the oxidized species reacts with one electron to give a radical form, which, in turn, is reduced and protonated to give NAD(P)H. However, the radicals obtained in the first step can combine leading to inactive dimers as a side product. Modification of the electrode surface by deposition of metal particles was used to increase the protonation rate of the NAD(P) radicals, but again not much of the active NAD(P)H remained after a few regenerative cycles.[34] The problems of direct electrochemical methods have been overcome by introducing an indirect regeneration pathway (**Figure 4B**) using mediators, which act as electron carriers and can transfer two electrons or one hydride ion in a single step. Unfortunately, it is still very difficult to find a redox mediator that can regenerate NAD(P)H effectively with high *TOF*s/*TN*s. Hence, attempts have been made to recycle the cofactors indirectly by coupling the electrochemical redox system with an enzymatic process (**Figure 4C**). Although the mediators and enzymes used are soluble and form a homogeneous system,

the electrodes and associated catalytic materials are solid and as such the process can be considered heterogeneous. This will be discussed further in a following section.

Photocatalytic Regeneration

Photocatalytic regeneration borrows the concept of photosynthesis in nature that utilizes light-harvesting systems (LHSs) for generating electrons and electron transport chains (ETCs) for migrating electrons to ferredoxin for further NAD(P)H regeneration. This method strongly relies on the development of high-performance photocatalysts. In this respect, a number of organic photosensitizers, inorganic semiconductors, as well as some new materials (*e.g.*, carbon nitride, C_3N_4) have been explored in the context of NAD(P)H regeneration. Commonly, organic photosensitizers exhibit better catalytic activity which are 3-100 times better than inorganic semiconductors, of which the synthesis processes are, unfortunately, often complicated and labor-consuming. In contrast, the new materials such as C_3N_4, which are very easy to synthesize show comparable activity to organic photosensitizers, and may be promising photocatalysts for NAD(P)H regeneration. Photocatalytic regeneration using solid catalysts is a heterogeneous process and will be discussed in a later section.

Heterogeneous Catalytic Regeneration

The origin of NAD(P)H regeneration is a reductive reaction from its oxidized form ($NAD(P)^+$). A reducing agent and a catalyst are needed to promote such a chemical transformation ($NAD(P)^+ \rightarrow$ NAD(P)H). Readily available hydrogen gas (preferably from a renewable source) can be a clean source for this purpose with protons as the sole release that can be further consumed in bioconversions, thus achieving 100% atom efficiency. **Figure 5** illustrates enzymatic (FDH) CO_2 reduction as an example, producing formic acid that can be further reduced to formaldehyde using formaldehyde dehydrogenase and methanol using alcohol dehydrogenase; both require NADH regeneration. Such H_2-driven cofactor NAD(P)H

regeneration exhibits clear advantages in terms of process simplicity and cleanliness. Heterogeneous catalysts (*e.g.,* supported metals) are well-established in activating hydrogen (over *e.g.,* Pt, Pd, Rh, Ru, Ni, Au and Ag) and promoting reduction reactions with the added benefit of facile downstream separation. It would appear to be a straightforward process yet there are few reports of selective reduction of NAD^+ using supported metals and hydrogen.[12] This review focuses on this method with detailed discussion in the penultimate section.

Table 1 compares all the critical components involved in the six categories of methods for the regeneration of NAD(P)H cofactor. It is clear that regeneration using heterogeneous catalysts fulfil all four criteria (*e.g.,* avoiding the use of water-soluble catalyst, organic sacrificial hydride donor, mediator and minimizing byproduct generation), showing great potential for cleaner processes. In the following sections, heterogeneous systems for NAD(P)H regeneration that include (i) immobilized biocatalysis (enzyme immobilization), (ii) immobilized homogeneous catalysis (organometallic complex immobilization), (iii) electrocatalysis, (iv) photocatalysis (using solid catalysts) and (v) heterogeneous catalysis (supported metal catalysts) will be summarized and discussed in detail.

IMMOBILIZED BIOCATALYSIS

For large-scale industrial operations, enzymatic regeneration of cofactor NAD(P)H is still preferred due to its high activity and use of mild operating conditions.[35] Several enzymes are capable of regenerating NAD(P)H, in the presence of sacrificial substrates; **Table 2** summarizes the characteristics of these enzymatic regeneration systems. However, similar to the synthetic homogeneous catalyst counterparts, soluble enzymes are difficult to recycle and reuse. Moreover, some of these systems also generate soluble byproducts (see **Table 2**) which require laborious downstream separation. In order to enhance the sustainability, as well as

reduce operational cost of these enzymatic regeneration systems, enzyme immobilization has been reported for use in cofactor regenerations.

There are many immobilization methods for enzymes available in the literature and immobilized enzymes are wildly used in industry for facilitating catalyst recycle and reuse.[36] In general, these methods can be classified by a few categories including; crosslinking, entrapment, physical adsorption on a carrier and chemical binding to a carrier (see **Figure 6**). Depending on the systems of interest, each method has its own positive and negative features. Numerous reviews with details of enzyme immobilization can be found in the literature. [36-38] It is commonly accepted that enzyme immobilization enhances recycle and reuse of enzymes, which are otherwise expensive. It also simplifies downstream separation or purification of products. In some cases, immobilized enzymes show higher stability and longer life time than free enzymes.[38] However, lower activity is generally observed with immobilized enzymes when compared with their free counterparts due to mass transfer constrains. With the benefits of both economy and sustainability, immobilized enzymes are still worth consideration as heterogeneous systems for cofactor regeneration. Indeed, use of immobilized enzymes for cofactor regeneration was reported as early as 1975 when Wykes *et al.* demonstrated a NADH regeneration system using immobilized ADH and lactate dehydrogenases (LDH) on cellulose.[39] The following provides some key examples of cofactor regeneration systems using immobilized enzymes.

Immobilized FDH

FDH converts formate (or formic acid) to CO_2 in the presence of a cofactor NAD^+.[40] It possesses one distinctive feature; CO_2 gas is the only byproduct and does not require separation so downstream product purification becomes simpler. However, CO_2 is a greenhouse gas whose release should be always treated cautiously. Immobilization of FDH

for cofactor regeneration has been demonstrated.[41,42] For example, NADH regeneration using entrapped FDH in a poly(vinyl alcohol) (PVA) hydrogel has been studied by measuring the CO_2 release kinetics.[41] FDH has also been immobilized on commercial polymer beads (Immobead 150) for NADH regeneration. However, the activity was found to drop to less than 70% after 10 cycles.[42] Immobilized FDH has also been shown active as an *in situ* cofactor regeneration system. Demir *et al.* reported a system for the transformation of hydroxyacetone to a chiral (*S*)-1,2-propanediol with *in situ* NADH regeneration using FDH immobilized on magnetic nanoparticles (Fe_2O_3). However, this system requires a His(6)-tagged FDH, which was not commercially available and had to be extracted from bacteria, for binding onto the amine-functionalized Fe_2O_3.[43] A continuous feed system for L-lactate synthesis from pyruvate with *in situ* NADH regeneration using FDH supported on alkylated chitosan layers has also been reported. The regeneration system was shown to be active after 2 weeks but with only 50% of the initial activity retained. Nonetheless, this "continuous" regeneration for cofactor demonstrated engineering advances in coupled system for the production of chiral products.[44]

Immobilized hydrogenase

Cofactor regeneration using immobilized hydrogenases have also been demonstrated recently.[14,15] The merit of using hydrogenases for regeneration is associated with the cleanliness; using gaseous H_2 as the sacrificial substrate with H^+ being the sole byproduct.[14] However, unlike FDH, hydrogenases for cofactor regeneration are not widely available commercially with solubility and stability being the main concerns. Immobilization of hydrogenases does improve their stability and enhance recycling. For example, soluble hydrogenase from *R. eutropha* has been immobilized on porous glass with a 15-fold improvement in enzyme half-life from 10 to >150 h. However, the immobilization yield was

only 23% and showed significant loss of enzyme.[40] The stability of immobilized soluble hydrogenase on a polymer methoxy-poly(ethylene) glycol (mPEG) has also been studied in organic solvents and ionic liquids.[45] Although it showed a 5-fold improvement in half-life from 0.1 to 0.5 h and retained 91% activity of the free enzyme, further improvement are still necessary in order to promote immobilized hydrogenases for use in large-scale synthesis.

Immobilized ADH and GLDH

The other two enzymes commonly used for NADH regeneration are ADH and glutamate dehydrogenase (GLDH). In both cases, sacrificial substrates (alcohol and L-glutamate respectively) are required but, unlike regeneration using FDH or hydrogenase, the byproducts (aldehyde and 2-ketoglutarate) may require further downstream separations. For example, immobilized GLDH on polystyrene particles has been used for NADH regeneration in a 3-step conversion of CO_2 to methanol.[46] The three enzymes for CO_2 conversion were co-immobilized on one support in order to simplify downstream separation but a stoichiometric supply of L-glutamate (3 mol for 1 mol of methanol produced) is required, leading to a significant amount of waste. On the other hand, use of immobilized ADH for NADH regeneration may present an advantage over other systems. Immobilized ADH has been used as a "bi-functional" catalyst for both conversion of aldehyde to chiral alcohol products and cofactor regeneration in a "coupled-substrate" system.[47] Nagayama *et al.* demonstrated the enantioselective reduction of prochiral 4-methyl-2-pentanone to chiral (*R*)-4-methyl-2-pentanol using immobilized ADH (physically adsorbed on glass beads), which was also used for cofactor regeneration using propanol as the sacrificial substrate.[47] For clean use of immobilized enzyme for cofactor regeneration, ADH and GLDH may not be the best candidate.

Whole cell immobilization

When the enzyme required lacks stability, immobilization of the whole cell without enzyme extraction/purification may be an option. Many enzymes are extracted from microbial cells such as bacteria and then purified but these two steps can cause significant losses as well as denaturation of the enzymes. As a result, whole cell immobilization may be carried out to facilitate recovery, recycling and reuse. Whole cell immobilization has also been used in cofactor regeneration. For instance, yeast cells have been immobilized on alginate fibers for NADH regeneration.[48] Although enzyme loss can be avoided, whole cell immobilization can cause side reactions because more than one type of enzymes are likely to be found in each cell, reducing the selectivity of the system. For chiral drug and fine chemical synthesis, whole cell immobilization may not be appropriate.

Immobilized cofactor

The high cost of cofactor is the driving force for establishing a regeneration process. This also leads scientists/engineers to consider immobilizing cofactors for efficient recovery and reuse. For example, Chen *et al.* have recently demonstrated immobilizing NADH cofactor on chitosan coated magnetic nanoparticles with 1-ethyl-3-(-3-dimethylaminopropyl) carbodiimide hydrochloride (EDC) and *N*-hydroxysuccinimide (NHS) linkers.[49] As such, the cofactor can be recovered using an external magnet. A similar approach for cofactor immobilization has also been introduced by Li *et al.* using non-magnetic nanoparticles.[50] Over 60% of the activity had been retained after 6 cycles. However, similar to enzyme immobilization, lower activity is likely to be observed from cofactor immobilization when compared with free cofactors due to slower mass transfer. Such loss needs to be compensated by recycling and reuse of cofactor.

IMMOBILIZED HOMOGENEOUS CATALYSIS

Similar to enzymes, synthetic homogeneous catalysts can be immobilized on a carrier. So far there has only been one example of using an immobilized organometallic complex on a support to form a heterogeneous and recyclable regeneration catalyst. Hollmann and coworkers[51] have immobilized Rh(III)-TsDPEN (an analogue of $[Cp^*Rh(bpy)(H_2O)]^{2+}$) onto surface functionalized poly(ethylene) sinter chips. The activity of this catalyst was approximately one order of magnitude lower than that of the soluble $[Cp^*Rh(bpy)(H_2O)]^{2+}$ (*TOF* of 2.5 h^{-1} *vs.* 36 h^{-1}), which was attributed to severe diffusion limitations, similar to observation from immobilized enzymes. The solid catalyst could be reused for at least 10 times but suffered an activity decrease (by ~50%). One advance from this system is that interaction between the organometallic catalyst and enzyme can be reduced, minimizing the extent of mutual deactivation. Although there are still several issues (*e.g.*, low activity, deactivation) to be addressed, this approach is a conceptually interesting move from soluble to insoluble organometallic complexes, which may reduce catalyst cost and deal with the incompatibility of metal complexes with some biocatalysts.

ELECTROCATALYSIS

Cofactor regeneration using electrochemical methods can also be viewed as a heterogeneous process. Bare electrodes made from mercury[52] and carbon materials[53] were used as first attempts to understand the kinetics and mechanisms of NAD(P)H regeneration. It was demonstrated by applying high cathodic potentials (*ca.* -1.6 V) that the formed radicals could be partially reduced to NAD(P)H, preventing the formation of inactive dimers (**Figure 7**). However, protonation of the radicals is not selective resulting in the formation of inactive 1,6-NAD(P)H side products.

Representative studies in direct electrochemical regeneration of cofactor NAD(P)H have been summarized in **Table 3**.[54-59] Conductive vanadia-silica xerogels were used by Park *et al.*[54] to increase the conductivity of the reaction medium. Regeneration of NADH was coupled to the production of L-glutamate catalyzed by GLDH, and the reaction was complete in 3 h with a *TTN* of 3300 with respect to NAD^+. It has been proven by Omanovic *et al.*[55-59] that the yield of active NADH regenerated strongly depends on the electrode material. A series of bare Au, bare Cu and Pt-modified Au (Pt-Au) electrodes were used first.[55] At high cathodic potentials (-1.1 V *vs.* Saturated Calomel Electrode (SCE)), the yield of active NADH obtained was 30% on Au, 52% on Cu and 63% on Pt-Au. This was explained by the fact that the hydrogen produced in the reduction reaction, enhanced the mass-transport flux of NAD^+ towards the cathode surface. A further increase in the cathodic potential using a glassy carbon electrode (-2.3 V *vs.* Mercurous Sulfate Electrode (MSE)) resulted in a higher yield of NADH (98%).[56] The same group has been able to further expand their studies in the usage of bare electrodes for the regeneration of NAD(P)H. This time a glassy carbon electrode was modified with electrochemically deposited Pt and nickel nanoparticles.[57] The role of Ni and Pt particles was to speed up the protonation process by providing active adsorbed hydrogen (Ni-H_{asd} and Pt-H_{ads}). Small average particle sizes (79 nm for Pt and 83 nm for Ni) and narrow particle size distributions were responsible for the enhanced performance of the electrode. In addition, results showed a 100% recovery of active NADH at more positive potentials (-1.5 V *vs.* MSE).

Product purity and NADH regeneration kinetics have been recently proven to depend not only on electrode potential but also on the electrode material itself, both controlling the H_{ads} surface coverage and the metal-hydrogen (M-H_{ads}) bond strength. It was further shown that a bare Ti electrode exhibited the highest yield of enzymatically active NADH (96%) at an even lower cathodic potential (-0.8 V *vs.* Normal Hydrogen Electrode (NHE)) compared to

unmodified Ni, Co and Cd cathodes.[58] In order to further investigate the effect of surface-modified electrodes, an Ir/Ru-oxide coating was prepared on a Ti plate.[59] Although Ir and Ru are known to offer a high M-H_{ads} bond strength, it was found that at a potential of -1.7 V *vs.* MSE only 88% of NADH were active. This was explained by the hydrogen evolution reactions (Eqs. 1 and 2) that compete with the NAD-radical protonation, hence decreasing the selectivity to NADH.

$$Ti\text{-}H_{ads} + H^+ + e^- \rightarrow H_2 + Ti \quad (1)$$

$$2Ti\text{-}H_{ads} \rightarrow H_2 + 2Ti \quad (2)$$

Problems associated with the direct electrochemical regeneration of NAD(P)H can be overcome by the application of redox catalysts or mediators.[34,60] In order to be efficient, mediators must fulfil the following criteria:[61]

- Ability to transfer two electrons or one hydride ion in only one step.
- Activation at potentials more positive than -0.9 V to prevent direct $NAD(P)^+$ reduction.
- High selectivity towards the enzymatically active NAD(P)H.
- Avoidance of electron transfer to the enzymatic substrate.

Representative work in indirect electrochemical regeneration of cofactor NAD(P)H has been given in **Table 4**.[62-67] Steckhan *et al.* have worked thoroughly on the elaboration of active organometallic redox mediators (*e.g.*, Rh complexes). A typical Rh organometallic mediator accepts two electrons at the surface of the electrode and by inserting a proton into its coordination sphere. The resulting hydride ion is then transferrable to the cofactor. One of the first substances to meet the above requirements was the (2,2'-bipyridyl)Rh complex.[62] It is worth pointing out that these "redox" mediators are similar in structure/nature to those synthetic homogeneous catalysts used for cofactor regenerations. This mediator was able to reduce cyclohexanone to cyclohexanol with a 26% conversion. However, low *TTN*s (2.9 with regard to cofactor, and 1.2 with regard to catalyst) were detected as the result of electrode

passivation by a layer of $[Rh(bpy_2)(H_2O)_2]Cl$ or $[Rh(bpy_2)(OH)_2]Cl$ deposited on the surface of the cathode. A few years later, a new generation of Rh complexes were developed.[63] It was possible by using the $Cp(Me)_5$ ligand to improve the performance of the mediator and obtain 70% conversion of pyruvate to D-lactate with an enantiomeric excess (ee) of 93.5%, and *TN*s of 7 for the cofactor and 14 for the mediator.[63]

Oxidized $NAD(P)^+$ cofactors were also reduced to NADH and NADPH using a (pentamethylcyclo-pentadienyl-2,2'-bipyridine aqua) Rh mediator in an electrochemical cell constituted of packed bed graphite particles as a working electrode.[64] It was found that the *TN* for the redox catalyst was affected by the size of the carbon particles. Using NAD^+ as cofactor, a *TTN* of 400 was achieved with 80-200 μm carbon particles, which was clearly better than 40 obtained with 200-400 μm particles. 99% of the produced NADH was enzymatically active. On the other hand, a *TTN* value of 200 was achieved for the 80-200 μm particles in the reduction of $NADP^+$.

Cp*[Rh(5,5'-methyl-2,2'-bipyridine)] **(1)** and Cp*[Rh(4,4'-methoxy-2,2'-bipyridine)] **(2)** complexes were able to reduce $NADP^+$ three times faster than the previous established mediators.[65] A *TOF* of 97 h^{-1} and a reduction rate of 116 mM d^{-1} were achieved using catalyst **(1)**, whereas a *TOF* of 113 h^{-1} and a reduction rate of 136 mM d^{-1} were observed using catalyst **(2)**.

Unfortunately, coupling the indirect electrochemical regenerative systems by Rh complexes to an enzymatic synthesis reaction can result in the deactivation of the enzyme,[63] a similar observation to "mutual deactivation" in synthetic homogeneous regeneration systems. A membrane electrochemical reactor (MER) was applied to overcome this limitation. Lutz *et al.*[66] successfully developed a stable electro-enzymatic process by means of an enzyme-catalyst separation. For this purpose, a polymeric mediator was synthesized by

polycondensation of 2,2'-pipyridine-4,4'-di-aldehyde and α,ω-functionalized amino polyethylene glycol. This prevents direct contact between mediator and enzyme. A 90% substrate conversion was observed. Nevertheless, this system allowed the recovery of 86% of the mediator, resulting in a *TTN* of 214. Minteer *et al.*[67] have recently made a useful contribution to the immobilization of redox catalysts in the regeneration of NADH. In this work, immobilization of the pyridine-Rh complex took place on multi-walled carbon nanotubes (MWCNs) by means of π-π stacking effect, in which an aromatic moiety is attached to the catalyst allowing the latter to strongly adsorb on the electrode surface. An exceptional average *TOF* of 3.6 s^{-1} was observed over 10 cycles using 2 mM of NAD^+.

Direct and indirect electrochemical regeneration of NAD(P)H have not been proven to give sufficient efficiency in cofactor regeneration. Moreover, as it was difficult to design a redox mediator/catalyst that meet all criteria mentioned previously, attempts have been made to couple the indirect electrochemical regenerative system with an enzymatic process.[34] Many examples can be found in the literature where various mediators such as organic methyl viologen, and flavins were assisted by enzymes such as reductase, lipoamide dehydrogenase (LipDH), diaphrose and hydrogenase.

Representative studies in enzyme-coupled indirect electrochemical regeneration of cofactor NAD(P)H have been summarized in **Table 5**.[68-74] Using cyclic dithiols as mediators along with LipDH as enzyme, Whitesides *et al.*[69] were able to obtain *TTN*s of 920 for NAD^+ and 13 for the enzyme, after the reaction was completed in 3.5 days. However, only 5% of the NADH remained active, indicating a low selectivity. Introducing other types of mediators, higher residual activities were detected. Coupling methyl viologen with LipDH resulted in 51% active NADH and 65% active LipDH. Moreover, 68% residual activity for the cofactor and

80% for the enzyme were observed in the reduction of $NADP^+$ by means of methyl viologen and ferrodoxin-NADP-reductase (FDR).[68]

In an attempt to produce (*R*)-manadelate from benzoylformate in the presence of benzoyl formate reducate (BFR), a methyl viologen mediator was used alongside diaphorase enzyme.[70] Although the reaction exhibited 80% conversion in 30 h, methyl viologen contributed to the loss of 50% of BFR activity after 6 d (days). Instead, the use of flavine adenine dinucleotide (FAD) resulted in a more stable BFR and a 95% conversion in 18 h.

Regeneration of NADH together with methyl viologen was also reported in the enzymatic reduction of ketones. Since it has been known that enzymes are affected by free methyl viologen in solution, immobilization of mediation components is good practice. Osa *et al.*[71] employed a poly(acrylic acid) layer-coated graphite felt electrode to immobilize the mediators. They were able to successfully reduce 2-methylcyclohexanone (49.8% conversion, 100% ee, and 91 $TTN_{Mediator}$) and 3-methylcyclohexanone (51.7% conversion, 93.1% ee and 94 $TTN_{Mediator}$) to the corresponding alcohols. On the other hand, Tzedakis *et al.*[72,73] have designed micro-reactors which rely on unmodified Au electrodes, FAD mediator and FDH enzyme, for the continuous regeneration of NADH. The first reactor adopts the principle of laminar-based flow which keeps the reactants close to the electrode and prevents any side reactions. This system was able to retain a 31% NADH yield and a 41% conversion of pyruvate to L-lactate with a *TN* of 75.6 h^{-1} for the cofactor.[72] The second is a filter-press micro-reactor that gave 80 h^{-1} as NAD^+ *TN*.[73] Immobilized FADs were used in combination with FDH enzyme for the production of L-lactate from pyruvate. This time the FAD mediators were fixed on a carbon cloth as an economical support that provides a high specific surface area. The modified electrode contributed to a 60% substrate conversion after 96 h reaction, compared to a 50% conversion after 120 h with the bare carbon cloth electrode.[74]

All in all, as it has been challenging to find an efficient and enzyme friendly electron carrier that can overcome the disadvantages of the direct electrochemical regeneration of NAD(P)H, researchers have attempted to use an enzyme along with the mediator to push the *TN*s up to industrial levels. Unfortunately, by doing so, complications of product recovery and separation have arisen, leaving this regeneration method requiring further studies and investigations.

PHOTOCATALYSIS (USING SOLID PHOTOCATALYSTS)

Nature hints at an alternative way to regenerate cofactor through the photosynthetic process where photo-excited electron transfer regenerates reducing power in the form of NAD(P)H, for a further Calvin cycle.[75] This process strongly relies on the light-harvesting system, involving two protein complexes (photosystem I and II),[76] and has inspired researchers to explore a diverse range of artificial photosensitizers, including proflavine,[77] diphenylalanine/porphyrin nanotubes,[78] chromophore-bonded graphene nanosheets,[79,80] cadmium sulfide (CdS),[81,82] titanium oxide (TiO_2),[83-85] carbon nitride (C_3N_4),[86-89] and so on[90-92] (**Table 6**[78-84,86-88,91]). Due to the limited but efficient species of electron donors (mainly TEOA) and electron mediators (M, mainly $[Cp^*Rh(bpy)H_2O]^{2+}$) involved in photcatalytic regeneration of NAD(P)H,[7,10] we feature here the recent advances in photosensitizers that have exerted superiority in the photocatalytic regeneration of NAD(P)H. Based on chemical composition, the current photosensitizers can be categorized into organic and inorganic types.

Organic photosensitizers

Archiving nature-derived photosensitizers (chlorophyll, proflavine, porphyrins, *etc*.) is a direct way for photo-excitation of electrons and subsequent regeneration of NAD(P)H.[77,91] Although showing high efficiency, most of these photosensitizers are small molecules, presenting drawbacks of structural instability and difficulty in photosensitizer reusability and

product/photosensitizer separation. Modifying and immobilizing organic photosensitizers onto larger-scale supports is a feasible strategy for their practical applications. Physical entrapment and chemical grafting are two key methods. Park and coworkers[91] are pioneers in applying the physical entrapment to immobilize organic photosensitizer. In brief, they encapsulated porphyrins (light-harvesting pigments) within a porous lignocellulosic support through *in situ* precipitation of porphyrins during lignocellulose coagulation, thus acquiring a light-harvesting synthetic wood (LSW) **(Figure 8A)**. During the photocatalytic regeneration of NADH, the porphyrin absorbs photonic energy to create high-energy electrons, which are then transferred to M (the mediator $[Cp^{*}Rh(bpy)H_2O]^{2+}$). The activated M further transfers hydride (H^-) to NAD^+ in a single step, achieving the regeneration of NADH. Meanwhile, a sacrificial electron donor of TEOA reduces the oxidized porphyrin to avoid its degradation. Park *et al.* also evaluated and compared six types of hydrophobic porphyrins with different metal centers and side groups **(Figure 8B)**, where the highest *TOF* of ~1.250 h^{-1} can be achieved with the photosensitizer having 5,10,15,20-tetrakis(3-hydroxyphenyl)porphyrin (mTHPP) groups.

Unlike the non-specific structural characteristics of lignocellulosic supports, self-assembled hierarchically structured materials often exhibit unexpected functions due to the complex mutual interactions between different moieties. Typically, tubular structures usually exhibit extraordinary performance in electron transfer, which can lower the hole-electron recombination rate. Based on this theory, Park and coworkers[78] synthesized diphenylalanine/porphyrin light-harvesting peptide nanotubes through incorporating porphyrin photosensitizer during the self-assembly of diphenylalanine. To further enhance the separation/transfer efficiency of excited electrons from porphyrin to M, Pt nanoparticles were deposited on the surface of the peptide nanotubes. The reduction potential at the cathodic peak current of the Pt-doped peptide nanotubes and M is, respectively, located at 1.2 and 0.7

V (*vs.* Ag/AgCl), where the energetic relationship between Pt-doped peptide nanotubes and M is similar to that found in visible-light harvesting system in nature (**Figure 9A and 9B**). In the presence of the Pt-doped peptide nanotubes, the cathodic current of M at its reduction potential was enhanced, confirming that the excited electrons from the nanotubes were transferred to M. The *TOF* of Pt-doped peptide nanotubes is ~1.780 h^{-1} **(Figure 9C)**, suggesting superiority of the tubular structure compared to the lignocellulosic support. This artificial photosensitizer was further applied for photocatalytic synthesis of L-glutamate from α-ketoglutarate, coupled with a cofactor regeneration process. The conversion yield (1.45 mM) of L-glutamate was 2.7 and 48.3 times higher than those acquired from the Pt-doped peptide nanotubes and the sole porphyrin photosensitizer monomers, respectively (**Figure 9D**).

As indicated, physical entrapment offers a simple way to immobilize small organic photosensitizers through manipulating the multiple weak interactions between photosensitizers and the support. Alternatively, chemical grafting provides a more delicate and versatile method for molecule engineering of photosensitizers. It is possible to activate the specific groups of either photosensitizers or supports and then trigger the coupling reaction. Chromophore-bonded graphene nanosheets developed by Baeg and coworkers are one example of the representative immobilized photosensitizers through chemical grafting (**Figure 10A**).[79,80] This immobilized photosensitizer integrates the superiority of the chromophore in visible-light harvesting and the excellent electron transfer property of graphene, offering high potential in the photocatalytic regeneration of NAD(P)H. For instance, Baeg *et al.* reported a graphene-based visible-light photosensitizer, termed as CCGCMAQSP, in which covalently bonded multianthraquinone substituted porphyrin (MAQSP) was combined with the "chemically converted graphene" (CCG). They also choose two other photosensitizers,[93] $W_2Fe_4Ta_2O_{17}$ and MAQSP, with lower photocurrent than

CCGCMAQSP for comparison. As expected, CCGCMAQSP exhibits the highest *TOF* of 0.375 h^{-1} during NADH regeneration (**Figure 10B**). Through density functional theory (DFT) calculation, the authors further confirm that the energy level differences between neighbored segments are aligned for electrons to transfer from MAQSP to the hydrogen reduction site *via* CCG. Similar to Pt-doped peptide nanotubes, CCGCMAQSP is further applied for coupling with enzymatic conversion CO_2 to formic acid by formate dehydrogenase (**Figure 10C**). Although some success has been achieved, Baeg and coworkers still wondered if better photocatalysts can be synthesized (**Figure 10D**). In their subsequent investigation, two chromophoric motifs, isatin and porphyrin (termed as IP), were combined for further grafting onto graphene nanosheets. The resultant CCG-IP exhibits a much higher *TOF* (0.642 h^{-1}, **Figure 10E**) by contrast with CCGCMAQSP. In addition to coupling this photosensitizer with single-enzyme catalysis, Baeg *et al.* also extensively incorporated CCG-IP and CCGCMAQSP into multi-enzyme system for methanol production from CO_2.[80] A methanol concentration of 11.21 μM was obtained on exposure of the CCG-IP based integrated system to visible light over 60 min (**Figure 10F**). In our opinion, this trial shows the possibility of applying photocatalytic regeneration of NAD(P)H in applications with more complicated reactions.

Although confronting many difficulties, "All-in-One" photocatalytic regeneration systems with integrated organic photosensitizer and mediator are still actively pursued. Knör and coworkers have performed very exciting work.[94,95] They synthesized a Rh-BipyE-PV*ab* polymer that contains bipyridine-containing poly-(arylene-ethynylene)-alt-poly(arylene-vinylene) copolymer (as photosensitizer) with a redox-active Rh cyclopentadienyl complex (as mediator) (**Figure 11A and 11B**). This Rh-BipyE-PV*ab* polymer is coated on glass beads for photocatalytic regeneration of NADH with formate or TEOA as the electron donor. Due to the integrated property of this photosensitizer, the photon absorption, electron generation

and transfer, and the NADH regeneration process all occur in one polymer chain. The amount of regenerated NADH gradually increased with extended reaction time (**Figure 11C**). However, these authors adopted an alternative index to evaluate the regeneration efficiency, which was calculated based on the surface area of the glass beads. The reaction rate can reach as high as 1.8 μmol cm^{-2} h^{-1}. Although we cannot compare this value with previous results, this Rh-BipyE-PV*ab* polymer shows superiority in many aspects. Specifically, in contrast to existing systems with molecule-sized Rh complexes, the Rh-BipyE-PV*ab* polymer works as both an immobilizing support and a photosensitizer, which can avoid the loss of mediator, and minimize the contact of catalyst with NADH-binding site of enzymes when applied in coupled photo-enzymatic catalytic systems.

Collectively, organic photosensitizers have shown high efficiency in photocatalytic regeneration of NAD(P)H (**Table 6**), although their molecule-scale nature seriously restricts further applications without proper immobilization. In this context, some researchers have already transferred their attention to inorganic photosensitizers with a particular structure, which is introduced in the following section.

Inorganic photosensitizer

As a typical inorganic photosensitizer, TiO_2 is the first choice for light-driven photocatalytic regeneration of NADH.[96] However, pristine TiO_2 has a band gap of ~3.2 eV, which means that electrons can only be excited by ultraviolet light (UV, accounting for only 4% of the sun's energy). More importantly, high-energy UV luminescence usually leads to rapidly increases in temperature that seriously harm biomolecules. Therefore, NAD(P)H regeneration systems enabled by pristine TiO_2 are inappropriate for coupling with enzymatic catalysis. Many efforts have been devoted to narrowing of the band gap through modifying TiO_2. Jiang and coworkers have contributed significantly in this area.[83-85] They explore a general strategy

of doping non-metal elements (including carbon, boron, nitrogen, phosphorus, *etc*.) to examine whether the doped element has this function. They initially synthesized carbon-doped TiO_2 through sol-gel process using titanium oxide with ethanol and acetic acid as carbon sources.[83] The carbon doping indeed narrows the band gap of TiO_2, causing a red shift of the absorption edge, and enhances the absorption of visible light. Under visible light irradiation, the carbon-doped TiO_2 exhibits high activity and selectivity towards enzymatic active NADH in the presence of M and the electron donor. Jiang *et al.* also investigated the influence of several factors, including electron donor species, pH, M concentrations, *etc*., on the regeneration efficiency of NADH. Phosphorus and nitrogen can also be doped in TiO_2,[84,85] and function similarly to carbon-doped TiO_2. Compared with organic photosensitizers as mentioned in the previous section, TiO_2-based photosensitizers exhibit a much lower *TOF* (0.031 h^{-1}) in NADH regeneration. But, as the first generation of heterogeneous inorganic photosensitizer, modified TiO_2 paves the way of developing other types of inorganic photosensitizers.

Quantum dot nanocrystals (including cadmium sulfide (CdS), zinc sulfide (ZnS), cadmium selenide (CdSe), *etc*.) are other inorganic photosensitizer after TiO_2, which are attractive visible-light-harvesting materials due to their suitable band gaps.[81,90,92] Considering the nanoscale of quantum dot nanocrystals, it is better to dope this highly efficient photosensitizer onto a larger-scale support, where silica is preferred. Through simple hydrolysis and the nucleation reactions of an alcoholic silica precursor, Park and coworkers[82] successfully deposited CdS quantum dots (band gap ~2.4 eV) on the surface of SiO_2 beads by a successive ionic layer adsorption reaction of $CdSO_4$ and Na_2S. Facilely altering the number of coating cycles can manipulate the amount of CdS nanoparticles formed on the SiO_2 surface. Not only does it act as a support, the SiO_2 can also interact with the metal center (Rh^{2+}) of M. The ionic affinity between the surface –OH groups of SiO_2 and the metal center of M may

boost the energy transfer between SiO_2 and M. Therefore, the photo-excited electrons from CdS could be transferred more efficiently to M. By using CdS-coated SiO_2 for visible-light-driven NADH regeneration, a high *TOF* of 0.278 h^{-1} is obtained, which is nearly ten times higher than that achieved with doped TiO_2.[82,83] Furthermore, owing to the heterogeneous nature of this photosensitizer, no significant decrease in activity is noted during four cycles of use. In terms of CdS-coated SiO_2, it is just speculated, not confirmed, that the interaction between M and SiO_2 support might exist and elevate the electron and energy transfer. This has stimulated researchers to fabricate more delicate structures for faster transfer of photo-excited electrons to M. Rational design of "charge steps" in the hetero-structured inorganic photosensitizers to lower the "hole-electron" recombination rate is a simple and popular way to facilitate the charge carrier migration process, by which the photo-excited electrons and holes can be driven to the opposite side of the hetero-junction interface thus inhibiting their recombination rates.[97] A typical example of a hetero-junction structure is the combination of two most popular inorganic photosensitizers, *i.e.*, TiO_2 and CdS through coating CdS nanoparticles onto anodized TiO_2 nanotube arrays.[81] An NADH regeneration experiment enabled by the CdS-coated TiO_2 (CdS-TiO_2) nanotubular film with TEOA as the electron donor has lots of advantages, including easy synthesis, morphology control, rapid charge separation, *etc*. Due to the ~0.2 V more negative position of the conduction band (CB) edge of CdS compared to TiO_2, photo-excited electrons can be rapidly injected from CdS to TiO_2, remarkably suppressing electron–hole recombination. Compared with the Rh-BipyE-PV*ab* polymer photosensitizer,[94] this isotype hetero-junction structured photosensitizer exhibits an extremely high reaction rate (240 μmol cm^{-2} h^{-1}). To further support the hypothesis that efficient charge separation in CdS-TiO_2 nanotubular film can enhance the efficiency of NADH photoregeneration, CdS-coated Al_2O_3 (CdS-Al_2O_3) nanotubular film were also prepared. Although comprising similar topological structures, the CdS-Al_2O_3 nanotubular

films exhibited much lower NADH regeneration efficiency and *TOF*, which is ascribed to a higher degree of charge recombination (**Figure 12**).

Similar to the Rh-BipyE-PV*ab* polymer developed by Knör and coworkers, an "All-in-One" photocatalytic NAD(P)H regeneration system has been constructed based on CdS. King and coworkers[92] directly adsorbed ferredoxin $NADP^+$-reductase (FNR) onto CdS nanocrystals. Through combination of superfast reduction rate of enzymatic catalysis and direct transfer of photo-excited electrons from CdS to FNR, the resultant FNR@CdS systems show a remarkable *TOF* of ~1440 h^{-1} (NADPH). Nonetheless, FNR only shows specificity for NADPH regeneration, meanwhile, the FNR@CdS system is not readily recycled due to the small particle size (< 10 nm). This study opens up an interesting way of elevating regeneration efficiency of cofactors through combining two general approaches: biocatalysis and photocatalysis.

Newly emerged photosensitizer: graphitic carbon nitride (g-C_3N_4)

In addition to modified TiO_2 and CdS, few other inorganic or semiconductors have been explored for visible-light-driven photocatalytic regeneration of NADH for a relatively long period. Fortunately, in recent years, a newly emerged photosensitizer, namely graphitic carbon nitride (g-C_3N_4), has elicited excitement in many research communities. Due to its facile synthesis, appealing electronic band structure (band gap, ~2.7 eV), high physicochemical stability, and "earth-abundant" nature,[98] g-C_3N_4 is viewed as the next generation visible-light photosensitizer. Moreover, as a conjugated polymer, g-C_3N_4 is commonly derived through thermal-induced polymerization of abundant nitrogen-rich precursors. Accordingly, the surface chemistry can be facilely modulated by means of surface engineering at the molecular level, while the structure/morphology can be easily regulated. Antonietti and coworkers[86-89] were the first researchers who come up with a strategy of

utilizing g-C_3N_4 to photocatalytically regenerate cofactors (**Figure 13A**). In the presence of M and the electron donor, the general process and mechanism of NADH regeneration is similar to that enabled by TiO_2, CdS and other organic photosensitizers. In brief, g-C_3N_4 generates electron–hole pairs under visible light irradiation. The as-generated high-energy electrons from g-C_3N_4 are then transferred and abstracted by M. Subsequently, M, bearing electrons, selectively regenerates NADH by transferring two electrons to NAD^+ followed by coupling with one proton and region-specific transfer to NAD^+. The NADH regeneration efficiency can reach nearly 100% with *TOF*s of 0.067-1.326 h^{-1} that depend on the structures. Most excitingly, g-C_3N_4 can also photocatalytically regenerate NADH in the absence of M. The authors attribute this phenomenon to the following aspects: NAD^+ can be attached to the surface of C_3N_4 through π-π stacking of the heptazine building blocks of the g-C_3N_4 and adenine subunit of the NAD^+, which leads to the direct transfer of photo-excited electrons to NAD^+ (**Figure 13B and 13C**).[88] However, due to the absence of M, the number of electrons transferred to NAD^+ is uncontrollable. As a result, the formation of NADH is non-specific, whereas the product usually contains some enzymatically inactive 1,6-NADH. The maximum NADH regeneration efficiency is only ~50% with a *TOF* of lower than 0.665 h^{-1}. However, the importance of this study is to offer a way of simply manipulating interactions between NADH and photosensitizers to acquire M-free NADH regeneration systems. Based on the above achievements, they have synthesized g-C_3N_4 with diverse morphologies, including diatom-mimic structure,[87] porous nanospheres,[88] porous nano-rods,[86] frustule-like carbon nitride array,[89] *etc*. The aim of the structure alternation is to enhance the light-harvesting capability, prolong the light retention time, and lower the hole-electron recombination rate. All of the above g-C_3N_4 are coupled with NADH-dependent enzymatic catalysis (including peroxidase, dehydrogenase, *etc*.), verifying the superiority and possibility of C_3N_4 in artificial photosynthesis. Regrettably, no further investigation regarding mediator-free NAD(P)H

regeneration systems enabled by g-C_3N_4 has been reported since 2014.

To summarize, the merits of photocatalytic regeneration of NAD(P)H cofactor are reflected in many aspects, of which the most attractive one is the conversion of visible light into chemical energy behaving like nature. Through rationale design and manipulation, light-harvesting capability can be strengthened, while the hole-electron recombination rate can be suppressed. The newly developed photosensitizers perform better and better in the NAD(P)H regeneration efficiency in terms of *TOF*. Recent efforts have been devoted to develop "All-in-One" photosensitizers, which integrate M within photosensitizers. Nonetheless, most of the current photosensitizers still exhibit lower *TOF*s than other regeneration methods and rely on TEOA as the electron donor. The generated oxidized TEOA in the product solution still complicates the final purification process.

HETEROGENEOUS CATALYSIS (SUPPORTED METAL CATALYSTS)

The use of supported metal heterogeneous catalysts for cofactor regeneration was recently reported by some of us.[12] In this section we will describe the work conducted and update with latest results. In order to establish the feasibility of NAD(P)H regeneration catalyzed by supported metals, the process was initially tested by screening a series of commonly used hydrogenation/reduction active catalysts including Al_2O_3 supported (5 wt%) Pt, Rh, Ru, Pd (commercial catalysts) and Ni (6 wt%, laboratory synthesized[99]). It was encouraging to notice (**Figure 14A**) that all of the above catalysts showed some activity towards NADH production from the reduction of NAD^+ by H_2 (see Wang and Yiu[12] for experimental details). Since Pt gave a continuous increase in NADH generation, a Pt catalyst of lower loading was investigated *i.e.,* 1 wt%, over both Al_2O_3 and carbon as carriers. A low loading is favorable for NADH regeneration (**Figure 14B**) where Pt/Al_2O_3 outperformed Au/Al_2O_3 (laboratory synthesized[100]; introduced for comparison purpose due to its chemoselectivity) in terms of

activity and Pt/C in terms of selectivity (the high initial activity of this catalyst is interesting and worthy of further investigation). The concentration of NADH (rather than its inactive isomer) was also confirmed independently by ^{1}H NMR analysis (**Figure 14B and Figure 15**), which was in good agreement with the result determined by UV spectrophotometry and demonstrated the heterogeneous catalyst promoted NADH regeneration. This encouraging observation should not be a complete surprise as supported Pt has shown activity in the hydrogenation of compounds with similar ring structure to NADH (*e.g.*, pyridines), and there are studies in the literature relating to photocatalytic and electrocatalytic regeneration using Pt nanoparticles as photosensitizer and proton carrier, respectively.

Taking Pt/Al_2O_3 (1 wt%) as the optimal catalyst, effects of reaction parameters (temperature, pH, pressure and catalyst pretreatment) were studied over extended times (*i.e.*, 6 h) in order to understand and optimize this innovative NADH regeneration process. As seen in **Figure 16**, under benchmark conditions (*i.e.*, 37 ℃, pH = 7 and 9 atm H_2) the regenerated NADH at the end of reaction achieved 100% selectivity towards the enzymatically active form (~50% yield) and this was confirmed by results from both ^{1}H NMR and an independent enzymatic assay (experimental details available from Wang and Yiu[12]). In general, high temperature, pH and H_2 pressure favor the reduction of NAD^+ to NADH (**Figure 17**), which can be related to the activation energy provided (from temperature), driven force for the forward reaction (neutralization of the H^+ produced, **Figure 5**) and increased H_2 solubility (more reactant available), respectively. Although these observations are promising, it is worth pointing out that high temperature (60 ℃) and prolonged reaction time (24 h) can lead to the formation of undesirable products and a loss of cofactor NADH **(Figure 17A)**. This tends not to be a problem and has little effect on an actual enzymatic reduction with *in situ* NADH recycling system because it is typically operated at ~37 ℃ or lower temperatures while excessive accumulation of cofactor can be prevented by its concurrent consumption by a substrate over

the production enzyme. The *TOF*s (all < 100 h^{-1}) obtained under various conditions are presented in **Figure 17**, suggesting further enhancement would be beneficial. It is also evident that the H_2 treated catalyst is more active than the as-received one **(Figure 17D)**, suggesting some differences in their structural characteristics.

Both the as received and H_2 treated catalysts have therefore been fully characterized and the results compiled in **Table 7**[12] and **Figure 18**. There are not significant differences in terms of surface area/porosity and Pt particle size/range (see **Figure 18A** and **18B** for representative STEM images and associated particle size distributions). The H_2 activation capacity evident from both catalysts may be responsible for the reduction of NAD^+, where the higher (~5 times) value obtained over the H_2 treated catalyst is consistent with the catalytic performance. The X-ray diffraction (XRD) patterns **(Figure 18C)** of the as received Pt/Al_2O_3 is characterised by peaks at $2\theta = 37.6°$, 39.5°, 45.9° and 67.0° corresponding to the (311), (222), (400) and (440) planes of cubic γ-Al_2O_3, respectively and a peak at $2\theta = 33.0°$ that is attributed to α-PtO_2 (100). After H_2 treatment at 350°C for 1h, the absence of α-PtO_2 (100) characteristic peak indicates the full reduction of Pt oxide species to metallic Pt. This is consistent with the H_2 TPR measurement, where two reduction peaks were observed at 205 and 350 ℃, respectively. The former low temperature signal can be linked to the reduction of bulk Pt oxide species (PtO_x) with week interaction with support Al_2O_3 while the high temperature one is resulted from Pt species (PtO_x or (hydroxyl)chlorided Pt) interacted strongly with Al_2O_3. This is consistent with the H_2 temperature programmed reduction (TPR) profile **(Figure 18D)** that the pretreatment at 350 ℃ (for 1 h) is sufficient to reduce all Pt oxide species. The increased H_2 uptake can therefore be linked to the further reduction of Pt species over the as received catalyst, suggesting metallic Pt (at least) contains the active site for this reaction. Dissociative activation of H_2 over Pt has been known for many years. The polarized H atom ($H^{\delta-}$) could easily lose an electron to the nicotinamide ring (likely to be the

adsorbed part of the molecule) whose further pronation may also be catalyzed by Pt metal at the same site.

The ultimate goal for NADH regeneration is to couple this *in situ* with the main enzymatic reaction, which can be challenging due to compatibility issues (as discussed previously in some systems involving organometallic complexes). We have therefore integrated NADH regeneration by Pt/Al_2O_3 with conversion of propanal to propanol over ADH as a model enzymatic redox transformation and the results are shown in **Figure 19**. In batch mode, the production of propanol is limited by the available NADH and without Pt/Al_2O_3 addition propanol yield reached an upper limit of 70%. Cofactor regeneration by Pt/Al_2O_3 extended alcohol production beyond the initial NADH/propanal stoichiometry to reach full conversion (100% yield, **Figure 19A**). Moreover, in order to realize the full potential of this *in situ* cofactor regeneration strategy the feasibility of fed-batch propanol production was investigated using a fixed starting amount of NADH with continuous propanal supply and cofactor regeneration by Pt/Al_2O_3. Without cofactor regeneration, propanol production is limited by the initial NADH concentration (**Figure 19B**). Propanol production with a continuous feed was achieved through the combined catalytic action of Pt/Al_2O_3 and alcohol dehydrogenase where a constant level of propanol production was maintained in operation for up to 100 h. This hybrid synthetic-biocatalytic system (with further enhancements considered) can serve as a new route for cleaner production of chemicals by NADH dependent enzymes. Prompted by this work, Vincent and coworkers have recently loaded Pt (at a rather high loading, *i.e.*, 20 wt%) onto a carbon support to replace hydrogenase and work in tandem with NAD^+ reductase for NADH regeneration, which has also been proven feasible.[15] This further suggests that supported metals can work with enzymes in “one-pot” and exhibit no mutual inhibition.

These results demonstrate the feasibility of conventional heterogeneous catalysts promoted NAD^+ reduction by H_2 for the regeneration of NADH, which can be integrated in tandem with a real biotransformation with compatibility. This sixth regeneration method could provide new considerations in both NAD(P)H regeneration technology and the research of heterogeneous catalysis for novel applications.

SUMMARY AND OUTLOOK

NAD(P)H is a critical cofactor that participates in a broad range of enzymatic reduction reactions of significant importance as gauged by he continuously growing global pharmaceutical market where a wide number of drugs (or crucial intermediates during production) rely heavily on bioreduction (mainly due to its enantioselectivity) using oxidoreductases as biocatalyst and NAD(P)H as reducing agent. Effective procedures to generate NAD(P)H are essential given the high cost of this component and this has been the driver for the large body of research which has evolved over the last 50 years. With this objective six methods of promoting the $NAD(P)^+$ to NAD(P)H transformation have been established, namely enzymatic, chemical, homogeneous catalytic, electrochemical, photocatalytic and heterogeneous catalytic approaches.

Regeneration using enzymes (notably FDH and GDH) is still the state-of-the-art method and currently the only one applicable at industrial scale. This is a consequence of their high *TTN*, selectivity to enzymatically active NAD(P)H and excellent compatibility when coupling *in situ* with bioreductions. In addition to the limitations of using enzymes (*e.g.*, relatively high cost and low stability), the generation of water soluble byproducts (or CO_2 release), the complexity of species/components involved (*e.g.*, sacrificial organic hydride donor and corresponding byproduct) and product/catalyst separation are concerns in terms of towards sustainability and responsible production. Highlighted in this review is the advancement of

heterogeneous systems for NAD(P)H regeneration across the six categories of methods for potential process simplicity, cleanliness and ease of downstream separation. With the exception of obsolete chemical regeneration using high redox potential salts, other approaches are (*e.g.,* electro- and heterogeneous catalysis) or could be designed/made (*e.g.,* enzymatic, homogeneous and photo- catalysis) to be heterogeneous. The category includes the immobilization of enzymes, organometallic complex and the use of solid photocatalysts. These heterogeneous processes unfortunately exhibit low activity in $NAD(P)^+$ reduction compared to the homogeneous methodologies with few examples reporting high *TOF*s. On the positive side, they have been shown to selectively catalyze NAD(P)H regeneration, enhance stability, facilitate recycling/separation and are compatible in general with *in situ* enzymatic reductions (with various successful examples).

Using heterogeneous catalytic systems do not directly simplify product separation as immobilized enzymes (and immobilized organic complex) still require sacrificial organic hydride donors while the performance of electrochemical and photocatalytic routes is strongly dependent on the use of toxic electron mediators in addition to hydride donors. A key improvement is the switch from organic hydride donors to H_2 (preferably from renewable resources) where protons are the only released species and can be consumed in the target biosynthesis (*i.e.,* achieving 100% atom efficiency). This makes immobilized hydrogenase and supported metal catalysts ideal candidates, both of which have been proven compatible with enzymatic reductions. Future research in improving the catalytic efficiency is important in fulfill the potential of these two methods in the cleaner production of drugs and chemicals. While the enzymatic (hydrogenase) process is relatively more established, the reaction mechanism of supported metals promoting $NAD(P)^+$ reduction is still unclear. An understanding of how $NAD(P)^+$ interacts with the catalyst surface, active sites, reaction pathways and energetics will contribute significantly to the rational design of effective

catalytic materials. It is hoped that cofactor NAD(P)H regeneration using H_2 over solid reagent can be developed to an industrially acceptable level in the future with interdisciplinary efforts from chemists, engineers, biologists and industrial partners.

AUTHOR CONTRIBUTIONS

X.W. conceived and proposed this work with support from H.H.P.Y. and R.F.H. The enzymatic, electrochemical and photocatalytic regeneration parts were performed mainly by H.H.P.Y., T.S. and J.S., respectively. X.W. performed the experimental work, wrote the remaining sections and was responsible for integrating all components of the article with support from H.H.P.Y., R.F.H. and J.A.A. All authors read, revised and approved the manuscript.

ACKNOWLEDGEMENTS

This work was supported by The Carnegie Trust for the Universities of Scotland (70265), The Royal Society (RG150001 and IE150611) and Scottish Carbon Capture and Storage (SCCS) program. J.S. also acknowledges financial support from The National Natural Science Foundation of China (21406163 and 91534126). T.S. was supported by a University of Aberdeen Elphinstone PhD Scholarship.

REFERENCES AND NOTES

1. Bornscheuer, U. T., Huisman, G. W., Kazlauskas, R. J., Lutz, S., Moore, J. C., and Robins, K. (2012) Engineering the third wave of biocatalysis. Nature *485*, 185-194.
2. Straathof, A. J. J. (2014) Transformation of biomass into commodity chemicals using enzymes or cells. Chem. Rev. *114*, 871-1908.
3. Ciriminna, R., and Pagliaro, M. (2013) Green chemistry in the fine chemicals and pharmaceutical industries. Org. Process. Res. Dev. *17*, 1479-1484.
4. Hollmann, F., Arends, I. W. C. E., and Holtmann, D. (2011) Enzymatic reductions for the chemist. Green Chem. *13*, 2285-2314.
5. EvaluatePharma. (2016) World Preview 2016, Outlook to 2022. (9th Edition), pp 9.

6. Gorecki, M. (2015) A configurational and conformational study of (-)-Oseltamivir using a multi-chiroptical approach. Org. Biomol. Chem. *13*, 2999-3010.
7. Wu, H., Tian, C., Song, X., Liu, C., Yang, D., and Jiang, Z. (2013) Methods for the regeneration of nicotinamide coenzymes. Green Chem. *15*, 1773-1789.
8. Faber, K. (2011) Biocatalytic Applications. in *Biotransformations in Organic Chemistry*, Springer, Berlin/Heidelberg. pp 31-313.
9. Hollmann, F., Arends, I. W. C. E., and Buehler, K. (2010) Biocatalytic redox reactions for organic synthesis: nonconventional regeneration methods. ChemCatChem *2*, 762-782.
10. Quinto, T., Köhler, V., and Ward, T. (2014) Recent trends in biomimetic NADH regeneration. Top. Catal. *57*, 321-331.
11. Poizat, M., Arends, I. W. C. E., and Hollmann, F. (2010) On the nature of mutual inactivation between $[Cp^*Rh(bpy)(H_2O)]^{2+}$ and enzymes–analysis and potential remedies. J. Mol. Catal. B: Enzym. *63*, 149-156.
12. Wang, X., and Yiu, H. H. P. (2016) Heterogeneous catalysis mediated cofactor NADH regeneration for enzymatic reduction. ACS Catal. *6*, 1880-1886.
13. Ni, Y., and Hollmann, F. (2016) Artificial photosynthesis: Hybrid systems. Adv. Biochem. Eng. Biotechnol., 1-22.
14. Lauterbach, L., Lenz, O., and Vincent, K. A. (2013) H_2-driven cofactor regeneration with $NAD(P)^+$-reducing hydrogenases. FEBS J. *280*, 3058-3068.
15. Reeve, H. A., Ash, P. A., Park, H., Huang, A., Posidias, M., Tomlinson, C., Lenz, O., and Vincent, K. A. (2017) Enzymes as modular catalysts for redox half-reactions in H_2-powered chemical synthesis: from biology to technology. Biochem. J. *474*, 215-230.
16. Liu, W., and Wang, P. (2007) Cofactor regeneration for sustainable enzymatic biosynthesis. Biotechnol. Adv. *25*, 369-384.
17. Goldberg, K., Schroer, K., Lütz, S., and Liese, A. (2007) Biocatalytic ketone reduction-a powerful tool for the production of chiral alcohols-part I: processes with isolated enzymes. Appl. Microbiol. Biotechnol. *76*, 237.
18. Weckbecker, A., Gröger, H., and Hummel, W. (2010) Regeneration of Nicotinamide Coenzymes: Principles and Applications for the Synthesis of Chiral Compounds. in *Biosystems Engineering I: Creating Superior Biocatalysts* (Wittmann, C., and Krull, R. eds.), Springer, Berlin/Heidelberg. pp 195-242.
19. van der Donk, W. A., and Zhao, H. (2003) Recent developments in pyridine nucleotide regeneration. Curr. Opin. Biotech. *14*, 421-426.

20. Wichmann, R., and Vasic-Racki, D. (2005) Cofactor Regeneration at the Lab Scale. in *Technology Transfer in Biotechnology: From lab to Industry to Production* (Kragl, U. ed.), Springer, Berlin/Heidelberg. pp 225-260.
21. Wandrey, C., and Wichmann, R. (1985) Coenzyme regeneration in membrane reactors. in *Enzymes and immobilized cells in biotechnology* (Laskin, A. I. ed.), Benjamin/Cummings Pub. Co., Menlo Park, CA. pp 177-208.
22. Chenault, H. K., and Whitesides, G. M. (1987) Regeneration of nicotinamide cofactors for use in organic synthesis. Appl. Biochem. Biotech *14*, 147-197.
23. Taylor, D. (2016) The Pharmaceutical Industry and the Future of Drug Development. in *Pharmaceuticals in the Environment* (Hester, R. E., and Harrison, R. M. eds.), The Royal Society of Chemistry, Cambridge. pp 1-33.
24. Rafter, G. W., and Colowick, S. P. (1957) Enzymatic preparation of DPNH and TPNH. Method. Enzymol. *3*, 887-890.
25. Calvin, S. J., Mangan, D., Miskelly, I., Moody, T. S., and Stevenson, P. J. (2012) Overcoming equilibrium issues with carbonyl reductase enzymes. Org. Process. Res. Dev. *16*, 82-86.
26. Jones, J. B., Sneddon, D. W., Higgins, W., and Lewis, A. J. (1972) Preparative-scale reductions of cyclic ketones and aldehyde substrates of horse liver alcohol dehydrogenase with in situ sodium dithionite recycling of catalytic amounts of NAD. Chem. Commun., 856-857.
27. Taylor, K. E., and Jones, J. B. (1976) Nicotinamide coenzyme regeneration by dihydropyridine and pyridinium compounds. J. Am. Chem. Soc. *98*, 5689-5694.
28. Raunio, R., and Lilius, E. (1971) Effect of dithionite on enzyme activities in vivo. Enzymologia *40*, 360.
29. Abril, O., and Whitesides, G. M. (1982) Hybrid organometallic/enzymic catalyst systems: regeneration of NADH using dihydrogen. J. Am. Chem. Soc. *104*, 1552-1554.
30. Maenaka, Y., Suenobu, T., and Fukuzumi, S. (2012) Efficient catalytic interconversion between NADH and NAD^+ accompanied by generation and consumption of hydrogen with a water-soluble iridium complex at ambient pressure and temperature. J. Am. Chem. Soc. *134*, 367-374.
31. Ganesan, V., Sivanesan, D., and Yoon, S. (2017) Correlation between the structure and catalytic activity of [Cp*Rh(substituted bipyridine)] complexes for NADH regeneration. Inorg. Chem. *56*, 1366-1374.
32. Bhaduri, S., Mathur, P., Payra, P., and Sharma, K. (1998) Coupling of catalyses by

carbonyl clusters and dehydrogenases: reduction of pyruvate to l-lactate by dihydrogen. J. Am. Chem. Soc. *120*, 12127-12128.

33. Canivet, J., Süss-Fink, G., and Štěpnička, P. (2007) Water-soluble phenanthroline complexes of rhodium, iridium and ruthenium for the regeneration of NADH in the enzymatic reduction of ketones. Eur. J. Inorg. Chem. *2007*, 4736-4742.
34. Kohlmann, C., Märkle, W., and Lütz, S. (2008) Electroenzymatic synthesis. J. Mol. Catal. B: Enzym. *51*, 57-72.
35. Vasic-Racki, D. (2006) History of Industrial Biotransformations–Dreams and Realities. in *Industrial Biotransformations* (Liese, A., Seelbach, K., and Wandrey, C. eds.), Wiley-VCH Verlag GmbH & Co. KGaA, Weinheim. pp 1-36.
36. Sheldon, R. A. (2011) Characteristic features and biotechnological applications of cross-linked enzyme aggregates (CLEAs). Appl. Microbiol. Biotechnol. *92*, 467-477.
37. Sheldon, R. A. (2007) Enzyme immobilization: The quest for optimum performance. Adv. Synth. Catal. *349*, 1289-1307.
38. Sheldon, R. A., and van Pelt, S. (2013) Enzyme immobilisation in biocatalysis: why, what and how. Chem. Soc. Rev. *42*, 6223-6235.
39. Wykes, J. R., Dunnill, P., and Lilly, M. D. (1975) Cofactor recycling in an enzyme reactor. A comparison using free and immobilized dehydrogenases with free and immobilized NAD. Biotechnol. Bioeng. *17*, 51-68.
40. Danielsson, B., Winqvist, F., Malpote, J. Y., and Mosbach, K. (1982) Regeneration of NADH with immobilized systems of alanine dehydrogenase and hydrogen dehydrogenase. Biotechnol. Lett. *4*, 673-678.
41. Ansorge-Schumacher, M. B., Steinsiek, S., Eberhard, W., Keramidas, N., Erkens, K., Hartmeier, W., and Büchs, J. (2006) Assaying CO_2 release for determination of formate dehydrogenase activity in entrapment matrices and aqueous-organic two-phase systems. Biotechnol. Bioeng. *95*, 199-203.
42. Binay, B., Alagöz, D., Yildirim, D., Çelik, A., and Tükel, S. S. (2016) Highly stable and reusable immobilized formate dehydrogenases: Promising biocatalysts for in situ regeneration of NADH. Beilstein J. Org. Chem. *12*, 271-277.
43. Demir, A. S., Talpur, F. N., Betul Sopaci, S., Kohring, G. W., and Celik, A. (2011) Selective oxidation and reduction reactions with cofactor regeneration mediated by galactitol-, lactate-, and formate dehydrogenases immobilized on magnetic nanoparticles. J. Biotechnol. *152*, 176-183.
44. Roche, J., Groenen-Serrano, K., Reynes, O., Chauvet, F., and Tzedakis, T. (2014)

NADH regenerated using immobilized FDH in a continuously supplied reactor – application to l-lactate synthesis. Chem. Eng. J. *239*, 216-225.

45. Ratzka, J., Lauterbach, L., Lenz, O., and Ansorge-Schumacher, M. B. (2012) Stabilisation of the NAD^+-reducing soluble [NiFe]-hydrogenase from Ralstonia eutropha H16 through modification with methoxy-poly(ethylene) glycol. J. Mol. Catal. B: Enzym. *74*, 219-223.
46. El-Zahab, B., Donnelly, D., and Wang, P. (2008) Particle-tethered NADH for production of methanol from CO_2 catalyzed by coimmobilized enzymes. Biotechnol. Bioeng. *99*, 508-514.
47. Nagayama, K., Spieß, A. C., and Büchs, J. (2012) Enhanced catalytic performance of immobilized Parvibaculum lavamentivorans alcohol dehydrogenase in a gas phase bioreactor using glycerol as an additive. Chem. Eng. J. *207–208*, 342-348.
48. Stevenson, E., Ibbotson, P. G., and Spedding, P. L. (1993) Regeneration of NADH in a bioreactor using yeast cells immobilized in alginate fiber: I. Method and effect of reactor variables. Biotechnol. Bioeng. *42*, 43-49.
49. Chen, G., Wu, Z., and Ma, Y. (2015) A novel method for preparation of MNP@CS-tethered coenzyme for coupled oxidoreductase system. J. Biotechnol. *196–197*, 52-57.
50. Li, Y., Liang, H., Sun, L., Wu, J., and Yuan, Q. (2013) Nanoparticle-tethered NAD^+ with in situ cofactor regeneration. Biotechnol. Lett. *35*, 915-919.
51. de Torres, M., Dimroth, J., Arends, I. W. C. E., Keilitz, J., and Hollmann, F. (2012) Towards recyclable NAD(P)H regeneration catalysts. Molecules *17*, 9835-9841.
52. Burnett, J. N., and Underwood, A. L. (1965) Electrochemical reduction of diphosphopyridine nucleotide. Biochemistry *4*, 2060-2064.
53. Schmakel, C. O., Santhanam, K. S. V., and Elving, P. J. (1975) Nicotinamide adenine dinucleotide (NAD^+) and related compounds. Electrochemical redox pattern and allied chemical behavior. J. Am. Chem. Soc. *97*, 5083-5092.
54. Siu, E., Won, K., and Park, C. B. (2007) Electrochemical regeneration of NADH using conductive vanadia-silica xerogels. Biotechnol. Progr. *23*, 293-296.
55. Damian, A., Maloo, K., and Omanovic, S. (2007) Direct electrochemical regeneration of NADH on Au, Cu and Pt-Au electrodes. Chem. Biochem. Eng. Q. *21*, 21-32.
56. Ali, I., Soomro, B., and Omanovic, S. (2011) Electrochemical regeneration of NADH on a glassy carbon electrode surface: The influence of electrolysis potential. Electrochem. Commun. *13*, 562-565.
57. Ali, I., Gill, A., and Omanovic, S. (2012) Direct electrochemical regeneration of the

enzymatic cofactor 1,4-NADH employing nano-patterned glassy carbon/Pt and glassy carbon/Ni electrodes. Chem. Eng. J. *188*, 173-180.

58. Ali, I., Khan, T., and Omanovic, S. (2014) Direct electrochemical regeneration of the cofactor NADH on bare Ti, Ni, Co and Cd electrodes: the influence of electrode potential and electrode material. J. Mol. Catal. A: Chem. *387*, 86-91.
59. Ullah, N., Ali, I., and Omanovic, S. (2015) Direct electrocatalytic reduction of coenzyme NAD^+ to enzymatically-active 1,4-NADH employing an iridium/ruthenium-oxide electrode. Mater. Chem. Phys. *149–150*, 413-417.
60. Chenault, H. K., Simon, E. S., and Whitesides, G. M. (1988) Cofactor regeneration for enzyme-catalysed synthesis. Biotechnol. Genet. Eng. Rev. *6*, 221-270.
61. Steckhan, E. (1994) Electroenzymatic synthesis. in *Electrochemistry V* (Steckhan, E. ed.), Springer, Berlin/Heidelberg. pp 83-111.
62. Wienkamp, R., and Steckhan, E. (1982) Indirect electrochemical regeneration of NADH by a bipyridinerhodium(i) complex as electron-transfer agent. Angew. Chem. Int. Ed. *21*, 782-783.
63. Ruppert, R., Herrmann, S., and Steckhan, E. (1987) Efficient indirect electrochemical in-situ regeneration of NADH: Electrochemically driven enzymatic reduction of pyruvate catalyzed by d-LDH. Tetrahedron Lett. *28*, 6583-6586.
64. Vuorilehto, K., Lütz, S., and Wandrey, C. (2004) Indirect electrochemical reduction of nicotinamide coenzymes. Bioelectrochemistry *65*, 1-7.
65. Hildebrand, F., Kohlmann, C., Franz, A., and Lütz, S. (2008) Synthesis, characterization and application of new rhodium complexes for indirect electrochemical cofactor regeneration. Adv. Synth. Catal. *350*, 909-918.
66. Hildebrand, F., and Lütz, S. (2009) Stable electroenzymatic processes by catalyst separation. Chem-Eur. J. *15*, 4998-5001.
67. Tan, B., Hickey, D. P., Milton, R. D., Giroud, F., and Minteer, S. D. (2015) Regeneration of the NADH cofactor by a rhodium complex immobilized on multi-walled carbon nanotubes. J. Electrochem. Soc. *162*, H102-H107.
68. DiCosimo, R., Wong, C.-H., Daniels, L., and Whitesides, G. M. (1981) Enzyme-catalyzed organic synthesis: electrochemical regeneration of NAD(P)H from NAD(P) using methyl viologen and flavoenzymes. J. Org. Chem. *46*, 4622-4623.
69. Shaked, Z. e., Barber, J. J., and Whitesides, G. M. (1981) Combined electrochemical/enzymic method for in situ regeneration of NADH based on cathodic reduction of cyclic disulfides. J. Org. Chem. *46*, 4100-4101.

70. Kim, M.-H., and Yun, S.-E. (2004) Construction of an electro-enzymatic bioreactor for the production of (R)-mandelate from benzoylformate. Biotechnol. Lett. *26*, 21-26.
71. Kashiwagi, Y., Yanagisawa, Y., Shibayama, N., Nakahara, K., Kurashima, F., Anzai, J., and Osa, T. (1997) Preparative, electroenzymatic reduction of ketones on an all components-immobilized graphite felt electrode. Electrochim. Acta *42*, 2267-2270.
72. Yoon, S. K., Choban, E. R., Kane, C., Tzedakis, T., and Kenis, P. J. A. (2005) Laminar flow-based electrochemical microreactor for efficient regeneration of nicotinamide cofactors for biocatalysis. J. Am. Chem. Soc. *127*, 10466-10467.
73. Cheikhou, K., and Tzédakis, T. (2008) Electrochemical microreactor for chiral syntheses using the cofactor NADH. AIChE J. *54*, 1365-1376.
74. Jayabalan, R., Sathishkumar, M., Jeong, E. S., Mun, S. P., and Yun, S. E. (2012) Immobilization of flavin adenine dinucleotide (FAD) onto carbon cloth and its application as working electrode in an electroenzymatic bioreactor. Bioresour. Technol. *123*, 686-689.
75. Magnuson, A., Anderlund, M., Johansson, O., Lindblad, P., Lomoth, R., Polivka, T., Ott, S., Stensjö, K., Styring, S., and Sundström, V. (2009) Biomimetic and microbial approaches to solar fuel generation. Acc. Chem. Res. *42*, 1899-1909.
76. Jordan, P., Fromme, P., Witt, H. T., Klukas, O., Saenger, W., and Krauß, N. (2001) Three-dimensional structure of cyanobacterial photosystem I at 2.5 Å resolution. Nature *411*, 909-917.
77. Nam, D. H., and Park, C. B. (2012) Visible light-driven NADH regeneration sensitized by proflavine for biocatalysis. ChemBioChem *13*, 1278-1282.
78. Kim, J. H., Lee, M., Lee, J. S., and Park, C. B. (2012) Self-assembled light-harvesting peptide nanotubes for mimicking natural photosynthesis. Angew. Chem. Int. Ed. *51*, 517-520.
79. Yadav, R. K., Baeg, J.-O., Oh, G. H., Park, N.-J., Kong, K.-j., Kim, J., Hwang, D. W., and Biswas, S. K. (2012) A photocatalyst–enzyme coupled artificial photosynthesis system for solar energy in production of formic acid from CO_2. J. Am. Chem. Soc. *134*, 11455-11461.
80. Yadav, R. K., Oh, G. H., Park, N.-J., Kumar, A., Kong, K.-j., and Baeg, J.-O. (2014) Highly selective solar-driven methanol from CO_2 by a photocatalyst/biocatalyst integrated system. J. Am. Chem. Soc. *136*, 16728-16731.
81. Ryu, J., Lee, S. H., Nam, D. H., and Park, C. B. (2011) Rational design and engineering of quantum-dot-sensitized TiO_2 nanotube arrays for artificial photosynthesis. Adv.

Mater. *23*, 1883-1888.

82. Lee, S. H., Ryu, J., Nam, D. H., and Park, C. B. (2011) Photoenzymatic synthesis through sustainable NADH regeneration by SiO_2-supported quantum dots. Chem. Commun. *47*, 4643-4645.
83. Jiang, Z., Lü, C., and Wu, H. (2005) Photoregeneration of NADH using carbon-containing TiO_2. Ind. Eng. Chem. Res. *44*, 4165-4170.
84. Shi, Q., Yang, D., Jiang, Z., and Li, J. (2006) Visible-light photocatalytic regeneration of NADH using P-doped TiO_2 nanoparticles. J. Mol. Catal. B: Enzym. *43*, 44-48.
85. Geng, J., Yang, D., Zhu, J., Chen, D., and Jiang, Z. (2009) Nitrogen-doped TiO_2 nanotubes with enhanced photocatalytic activity synthesized by a facile wet chemistry method. Mater. Res. Bull. *44*, 146-150.
86. Liu, J., Huang, J., Zhou, H., and Antonietti, M. (2014) Uniform graphitic carbon nitride nanorod for efficient photocatalytic hydrogen evolution and sustained photoenzymatic catalysis. ACS Appl. Mater. Interfaces *6*, 8434-8440.
87. Liu, J., and Antonietti, M. (2013) Bio-inspired NADH regeneration by carbon nitride photocatalysis using diatom templates. Energy Environ. Sci. *6*, 1486-1493.
88. Huang, J., Antonietti, M., and Liu, J. (2014) Bio-inspired carbon nitride mesoporous spheres for artificial photosynthesis: photocatalytic cofactor regeneration for sustainable enzymatic synthesis. J. Mater. Chem. A *2*, 7686-7693.
89. Liu, J., Cazelles, R., Chen, Z. P., Zhou, H., Galarneau, A., and Antonietti, M. (2014) The bioinspired construction of an ordered carbon nitride array for photocatalytic mediated enzymatic reduction. Phys. Chem. Chem. Phys. *16*, 14699-14705.
90. Dibenedetto, A., Stufano, P., Macyk, W., Baran, T., Fragale, C., Costa, M., and Aresta, M. (2012) Hybrid technologies for an enhanced carbon recycling based on the enzymatic reduction of CO_2 to methanol in water: chemical and photochemical NADH regeneration. ChemSusChem *5*, 373-378.
91. Lee, M., Kim, J. H., Lee, S. H., Lee, S. H., and Park, C. B. (2011) Biomimetic artificial photosynthesis by light-harvesting synthetic wood. ChemSusChem *4*, 581-586.
92. Brown, K. A., Wilker, M. B., Boehm, M., Hamby, H., Dukovic, G., and King, P. W. (2016) Photocatalytic regeneration of nicotinamide cofactors by quantum dot–enzyme biohybrid complexes. ACS Catal. *6*, 2201-2204.
93. Park, C. B., Lee, S. H., Subramanian, E., Kale, B. B., Lee, S. M., and Baeg, J.-O. (2008) Solar energy in production of l-glutamate through visible light active photocatalyst—redox enzyme coupled bioreactor. Chem. Commun., 5423-5425.

94. Oppelt, K. T., Gasiorowski, J., Egbe, D. A. M., Kollender, J. P., Himmelsbach, M., Hassel, A. W., Sariciftci, N. S., and Knör, G. (2014) Rhodium-coordinated poly(arylene-ethynylene)-alt-poly(arylene-vinylene) copolymer acting as photocatalyst for visible-light-powered NAD^+/NADH reduction. J. Am. Chem. Soc. *136*, 12721-12729.
95. Oppelt, K. T., Wöß, E., Stiftinger, M., Schöfberger, W., Buchberger, W., and Knör, G. n. (2013) Photocatalytic reduction of artificial and natural nucleotide co-factors with a chlorophyll-like tin-dihydroporphyrin sensitizer. Inorg. Chem. *52*, 11910-11922.
96. Schneider, J., Matsuoka, M., Takeuchi, M., Zhang, J., Horiuchi, Y., Anpo, M., and Bahnemann, D. W. (2014) Understanding TiO_2 photocatalysis: mechanisms and materials. Chem. Rev. *114*, 9919-9986.
97. Eley, C., Li, T., Liao, F., Fairclough, S. M., Smith, J. M., Smith, G., and Tsang, S. C. E. (2014) Nanojunction-mediated photocatalytic enhancement in heterostructured CdS/ZnO, CdSe/ZnO, and CdTe/ZnO nanocrystals. Angew. Chem. Int. Ed. *53*, 7838-7842.
98. Ong, W.-J., Tan, L.-L., Ng, Y. H., Yong, S.-T., and Chai, S.-P. (2016) Graphitic carbon nitride (g-C_3N_4)-based photocatalysts for artificial photosynthesis and environmental remediation: Are we a step closer to achieving sustainability? Chem. Rev. *116*, 7159-7329.
99. Wang, X., Hao, Y., and Keane, M. A. (2016) Selective gas phase hydrogenation of p-nitrobenzonitrile to p-aminobenzonitrile over zirconia supported gold. Appl. Catal. A: Gen. *510*, 171-179.
100. Li, M., Wang, X., Perret, N., and Keane, M. A. (2014) Enhanced production of benzyl alcohol in the gas phase continuous hydrogenation of benzaldehyde over Au/Al_2O_3. Catal. Commun. *46*, 187-191.

Tables:

Table 1. Typical Main Criteria Required for Cofactor NAD(P)H Regeneration

Method	Recycling catalyst (ease of separation)	Avoiding organic sacrificial electron donor	Avoiding mediator	Clean production without byproduct
Enzymatic	× ✓ (immobilized enzyme)	× ✓ (using H_2)	✓	× ✓ (producing H^+)
Chemical	− (no catalyst)	✓ (inorganic)	✓	×
Homogeneous Catalytic	×	× ✓ (using H_2)	×	× ✓ (producing H^+)
Electrochemical	✓	✓	× ✓ (nonselective)	× ✓(using mediator)
Photocatalytic	× (organic photosensitizers) ✓(inorganic photosensitizers)	× ✓ (using H_2O)	× ✓ (C_3N_4, only 1 example)	×
Heterogeneous Catalytic	✓	✓ (using H_2)	✓	✓ (producing H^+)

Table 2. Characteristics of Enzymes Used in Cofactor NAD(P)H Regeneration

Enzyme	Substrate(s)	Byproduct(s) from regeneration	Advantages	Disadvantages
Alcohol dehydrogenase (ADH)	2-propanol (or other oxidizable alcohols)	Acetone (correspondent ketones/aldehydes)	• High activity • Low cost	• Water soluble byproducts requiring downstream separation
Formate dehydrogenase (FDH)	Formate/formic acid	CO_2	• No soluble byproducts • Enhanced product separation	• Low activity • CO_2 release
Glucose dehydrogenase (GDH)	Glucose	D-glucono-1,5-lactone	• High activity	• High cost • Water soluble byproducts requiring downstream separation
Glutamate dehydrogenase (GLDH)	Glutamate/glutamic acid	γ-aminobutyric acid	• Low cost	• Low activity • Water soluble byproducts requiring downstream separation
Hydrogenase	H_2	H^+	• Clean byproducts (H^+)	• Low stability compared with other enzymes • Commercial availability

Table 3. Direct Electrochemical Regeneration of Cofactor NAD(P)H

Electrode	Potential (V)	Cofactor	Key results
Pt using vanadia-silica xerogels[54]	2[a]	NAD^+	NADH yield = 100%; α-ketoglutarate conversion = 100%
Au[55]	-1.1 vs SCE[b]	NAD^+	NADH yield = 30%
Cu[55]	-1.2 vs SCE[b]	NAD^+	NADH yield = 52%
Pt-Au[55]	-1.1 vs SCE[b]	NAD^+	NADH yield = 63%
GC[56]	-2.3 vs MSE[c]	NAD^+	NADH yield = 98%
GC-Pt[57]	-1.6 vs MSE[c]	NAD^+	NADH yield = 100%
GC-Ni[57]	-1.5 vs MSE[c]	NAD^+	NADH yield = 100%
Ti[58]	-0.8 vs NHE[d]	NAD^+	NADH yield = 96%
Ni[58]	-1.3 vs NHE[d]	NAD^+	NADH yield = 92%
Co[58]	-0.9 vs NHE[d]	NAD^+	NADH yield = 82%
Cd[58]	-1.5 vs NHE[d]	NAD^+	NADH yield = 93%
Ir-Ru/Ti[59]	-1.7 vs MSE[c]	NAD^+	NADH yield = 88%

[a]2 V electricity applied.

[b]Saturated Calomel Electrode.

[c]Mercurous Sulfate Electrode.

[d]Normal Hydrogen Electrode.

Table 4. Indirect Electrochemical Regeneration of Cofactor NAD(P)H

Electrode	Potential (V)	Redox Catalyst/Mediator	Cofactor	Key results
Carbon foil[62]	-0.7 vs Ag/AgCl	$[Rh(bpy)_3]^{2+}$	NAD^+	Cyclohexanone conversion = 26%; $TTN_{Cofactor}$[a] = 2.9; $TTN_{Catalyst}$[b] = 1.2
Carbon foil[63]	-0.6 vs Ag/AgCl	$[Cp(Me)_5Rh(bipy)Cl]^+$	NAD^+	Pyruvate conversion = 70%; ee = 93.5%; $TTN_{Cofactor}$[a] = 14; $TTN_{Catalyst}$[b] = 7
Glassy carbon particles[64]	-0.5 vs NHE	(pentamethylcyclo-pentadienyl-2,2'-bipyridine aqua) Rh	NAD^+	NADH yield = 99.5%; $TTN_{Catalyst}$[b] = 400
			$NADP^+$	NADPH yield = 99.5%; $TTN_{Catalyst}$[b] = 200
Carbon felt[65]	-0.756 vs Ag/AgCl	Cp[Rh(5,5'-methyl-2,2'-bipyridine)]	$NADP^+$	$r_{reduction}$ = 116 mM d^{-1}; *TOF* = 97 h^{-1}
	-0.757 vs Ag/AgCl	Cp[Rh(4,4'-methoxy-2,2'-bipyridine)]	$NADP^+$	$r_{reduction}$= 136 mM d^{-1}; *TOF* = 113 h^{-1}
Glassy carbon[66]	-0.8 vs Ag/AgCl	Rh complex polymer	$NADP^+$	*p*-chloroacetophenone conversion = 90%; ee > 97.3%; $TTN_{Catalyst}$[b] = 214
MWCNs[67]	-0.75 vs SCE	Rh complex with a pyrene-substituted phenanthroline ligand	NAD^+	*TOF* = 3.6 s^{-1} (over 10 regeneration cycles)

[a]Cofactor total turnover number (mol of product produced per mol of cofactor used).

[b]Catalyst total turnover number (mol of product produced per mol of catalyst used).

Table 5. Enzyme-coupled Indirect Electrochemical Regeneration of Cofactor NAD(P)H

Electrode	Potential (V)	Mediator	Enzyme	Cofactor	Key results
Coiled W wire[68]	-0.72 vs SCE	Methyl viologen	LipDH	NAD^+	$TTN_{Cofactor}$[a] = 940; TTN_{Enzyme}[b] = 540,000
			FDR	$NADP^+$	$TTN_{Cofactor}$[a] = 1000; TTN_{Enzyme}[b] = 750,000
Coiled W wire[69]	-1 vs SCE	Dithiols (DTT)	LipDH	NAD^+	$TTN_{Cofactor}$[a] = 920; TTN_{Enzyme}[b] = 13
Modified graphite[70]	-0.8 vs SCE	Methyl viologen	Diaphorase	NAD^+	Benzoylformate conversion = 95% Benzoylformate conversion = 80% (50% loss of MV activity after 6 d)
Au amalgam[71]	-0.5 vs Ag/AgCl	Flavine adenine dinucleotide (FAD)	Diaphorase	NAD^+	2-methylcylohexanone conversion = 49.8%; ee = 100%; $TTN_{Mediator}$[c] = 91
	-0.7 vs Ag/AgCl	Methyl viologen			3-methylcyclohexanone conversion = 51.7%; ee = 93.1%; $TTN_{Mediator}$[c] = 94
Au[72]	-0.55 vs Pt	Flavine adenine dinucleotide (FAD)	FDH	NAD^+	NADH yield = 31%; Pyruvate conversion = 41%; TN = 75.6 h^{-1}.
Au[73]	-0.6 vs Pt				NADH yield = 50%; Pyruvate conversion = 20%; TN = 80 h^{-1}.
Unmodified carbon cloth[74]	-0.45 vs Ag/AgCl	Flavine adenine dinucleotide (FAD)	FDH	NAD^+	Pyruvate conversion = 50%
Modified carbon cloth[74]	-0.45 vs Ag/AgCl	Immobilized FAD			Pyruvate conversion = 60%

[a]Cofactor total turnover number (mol of product produced per mol of cofactor used).
[b]Enzyme total turnover number (mol of product produced per mol of enzyme used).
[c]Mediator total turnover number (mol of product produced per mol of mediator used).

Table 6. Photocatalytic Regeneration of Cofactor NAD(P)H by Selective Heterogeneous Photosensitizers: Summary of Reaction Conditions and Catalytic Performance

Photosensitizer	Electron donor	Mediator[a]	λ (nm)	pH	Yield (%)	*TOF* (h^{-1})
Light-harvesting synthetic wood[91]	TEOA	yes	≥ 400	7.4	4.30	1.250
Pt-doped peptide nanotubes[78]	TEOA	yes	≥ 400	6.0	17.80	1.780
CCGCMAQSP[79]	TEOA	yes	≥ 420	7.0	45.54	0.375
CCG-IP[80]	TEOA	yes	≥ 420	7.0	38.99	0.642
Rh-BipyE-PV*ab* polymer[94]	TEOA	yes	≥ 390	8.9	21.00	1.8[b]
Carbon-doped TiO_2[83]	Mercaptoethanol	yes	≥ 400	6.5	74.30	0.031
	H_2O	yes	≥ 400	6.0	63.98	0.011
Phosphorus-doped TiO_2[84]	H_2O	yes	≥ 400	6.5	34.60	0.006
CdS-coated SiO_2[82]	TEOA	yes	≥ 420	7.5	70.00	0.278
CdS-TiO_2 nanotubular film[81]	TEOA	yes	≥ 420	7.5	75.20	240[b]
Diatom-mimic structure (g-C_3N_4)[87]	TEOA	yes	≥ 420	8.0	100	0.067
	TEOA	no	≥ 420	10.0	50.00	0.248
Porous nanospheres (g-C_3N_4)[88]	TEOA	yes	≥ 420	8.0	100	1.326
	TEOA	no	≥ 420	10.0	50.00	0.665
Porous nanorods (g-C_3N_4)[86]	TEOA	yes	≥ 420	8.0	72.00	0.478

[a]$[Cp^*Rh(bpy)H_2O]^{2+}$, showing high specificity to enzymatically active NAD(P)H.

[b]The unit of these values is μmol cm^{-2} h^{-1}.

Table 7. Physicochemical Characteristics of Pt/Al_2O_3[12]

	Pt/Al_2O_3 (as received)	Pt/Al_2O_3 (H_2 treated)
BET surface area ($m^2\ g^{-1}$)	162	175
Total pore volume ($cm^3\ g^{-1}$)	0.40	0.43
Average pore size (nm)	7.8	8.0
Pt size range (nm)	0-7	0-10
d_{STEM} (nm)	2.2	3.4
H_2 chemisorption ($\mu mol\ g^{-1}$)	4.1	21.5

Figures:

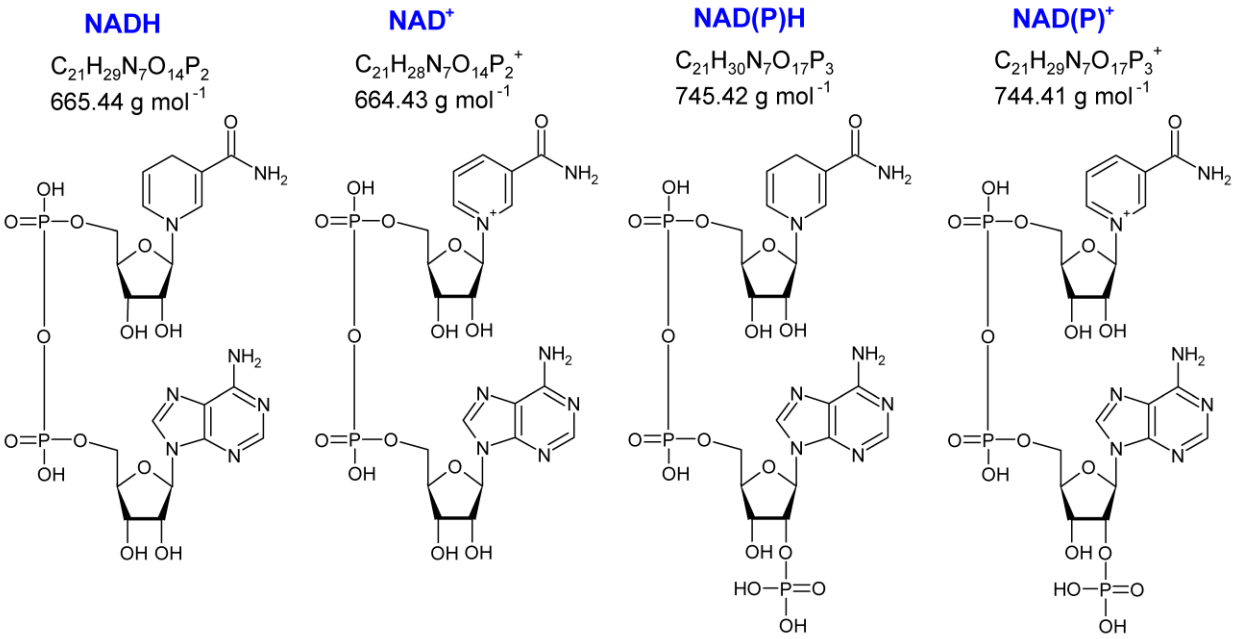

Figure 1. Molecular Structures of Nicotinamide Adenine Dinucleotide Cofactors

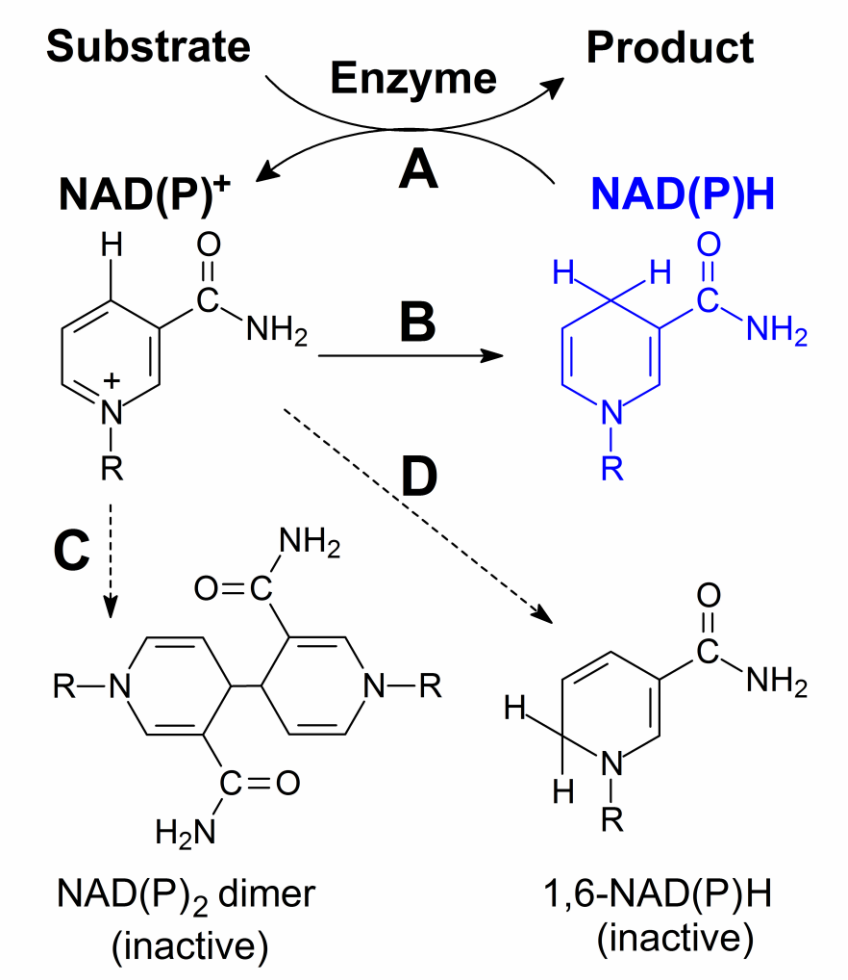

Figure 2. Schematic Representation of Enzymatic Reaction using Cofactor NAD(P)H and Possible Products Obtained from NAD(P)H Regeneration

(A) NAD(P)H consumption in biotransformation.

(B) Target pathway for NAD(P)H regeneration.

(C) Formation of (dashed arrows) enzymatically inactive $NAD(P)_2$ dimer.

(D) Formation of (dashed arrows) enzymatically inactive 1,6-NAD(P)H.

R indicates adenosine diphosphoribose.

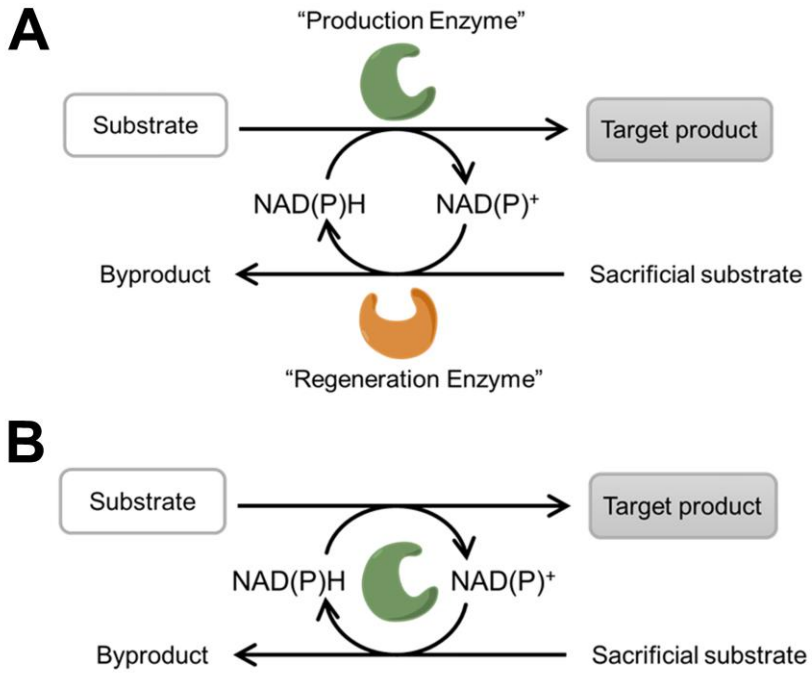

Figure 3. Schematic Representation of NAD(P)H Enzymatic Regeneration

(A) Coupled-enzyme approach.

(B) Coupled-substrate approach.

R indicates adenosine diphosphoribose.

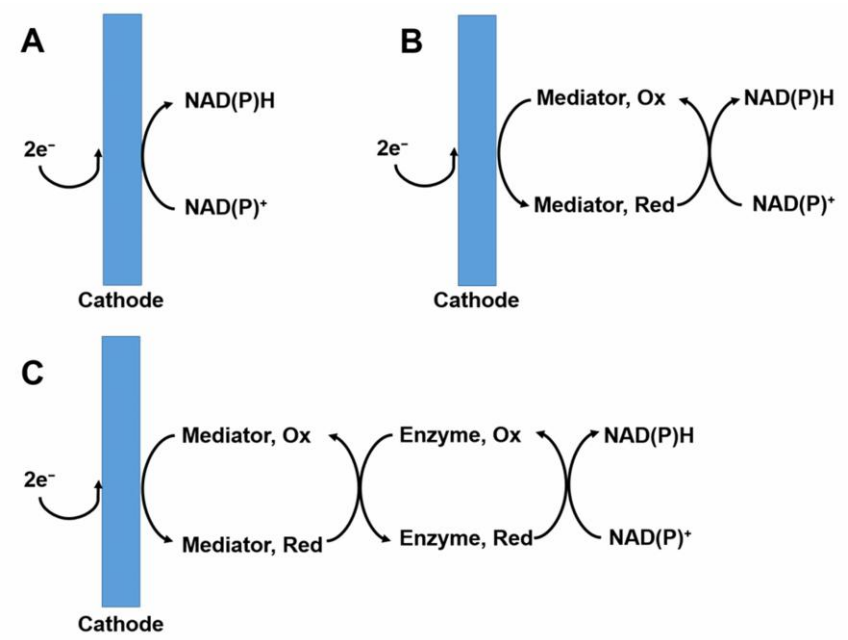

Figure 4. Schematic Representation of NAD(P)H Electrochemical Regeneration

(A) Direct electrochemical regeneration.

(B) Indirect electrochemical regeneration.

(C) Enzyme-coupled electrochemical regeneration.

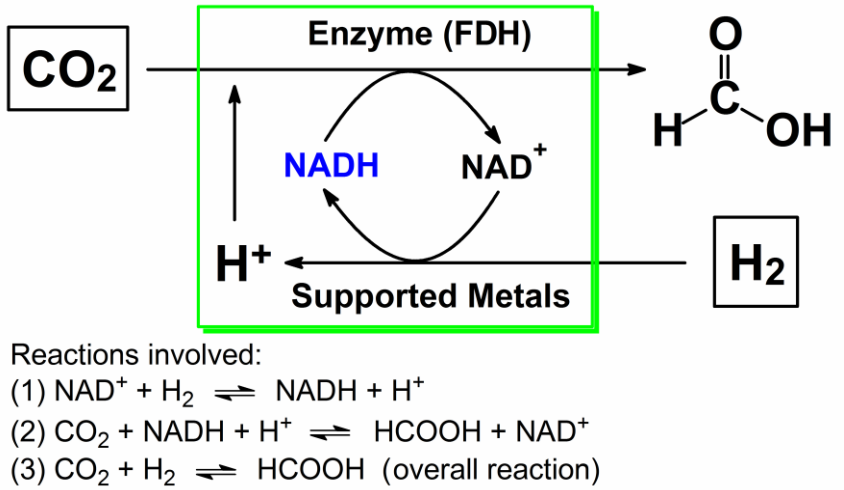

Figure 5. Schematic Representation of Coupling Heterogeneous Catalysts Promoting NADH Regeneration in Tandem with Enzymatic Reduction Using CO_2 as A Representative Substrate (Producing Formic Acid)

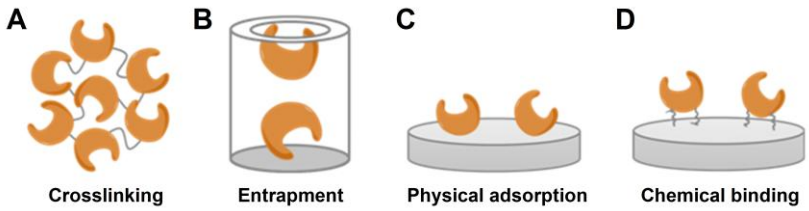

Figure 6. Methods for Enzyme Immobilization

(A) Crosslinking

(B) Entrapment

(C) Physical adsorption

(D) Chemical binding

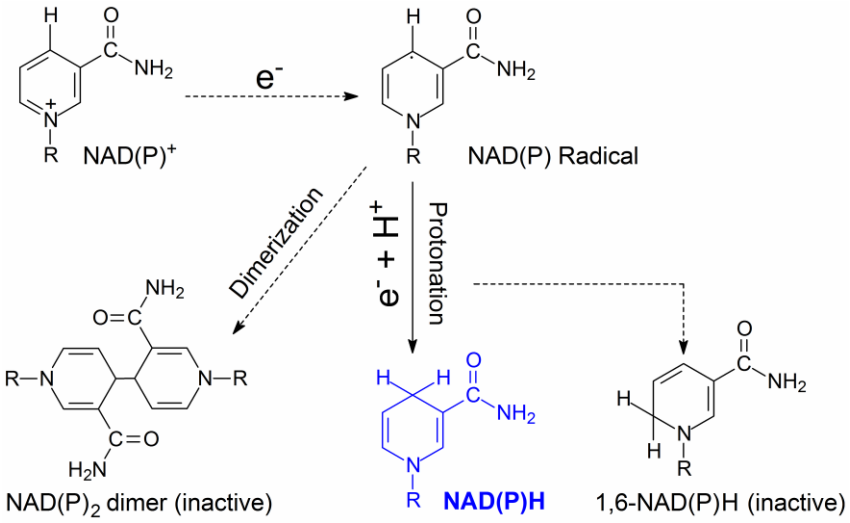

Figure 7. Reaction Pathways in Electrochemical Reduction of $NAD(P)^+$ to NAD(P)H.
R indicates adenosine diphosphoribose.

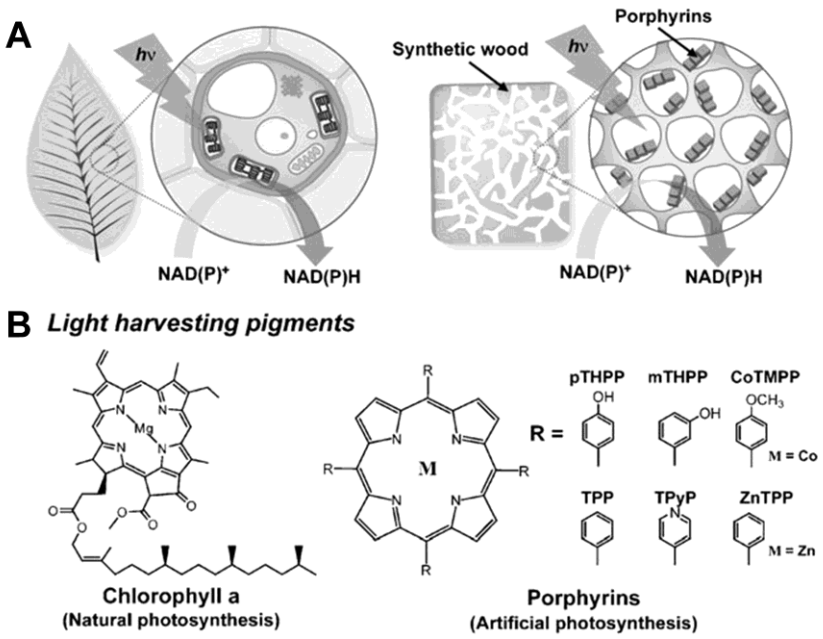

Figure 8. Schematic Illustration of Natural Photosynthesis and Artificial Systems with the Structure of Active Compounds

(A) Schematic illustration of the light-harvesting system in green plants (left) and light-harvesting synthetic wood (LSW) (right).

(B) Molecular structures of light-harvesting pigment in green plants (left) and LSW (right). Adapted from Lee *et al*.[91] with permission from the 2011 John Wiley & Sons Inc.

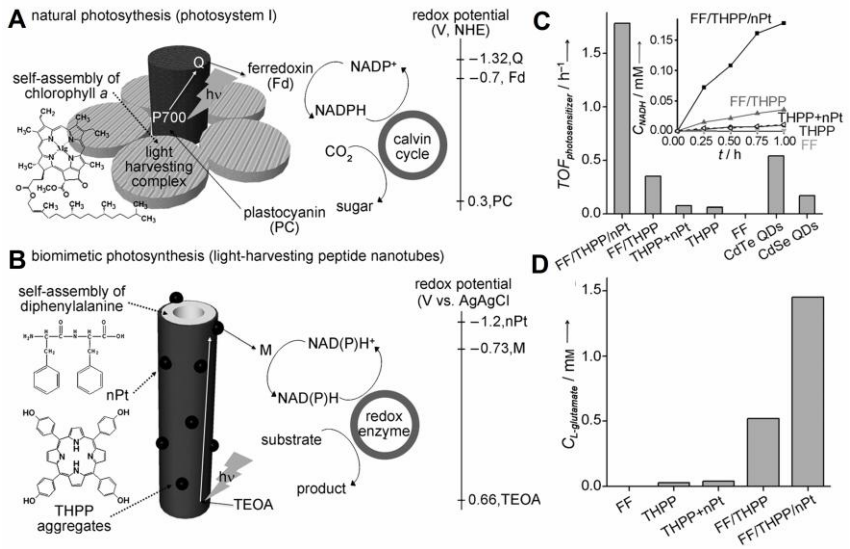

Figure 9. Schematic Illustration of Natural Photosynthesis and Artificial Systems with Associated Catalytic Performance

(A) Structure, biocatalytic reaction, and redox potential of natural photosynthesis by photosystem I.

(B) Artificial photosynthesis by light-harvesting Pt-doped peptide nanotubes.

(C) Turnover frequency (*TOF*) of different types of nanotubes in comparison with other inorganic photosensitizers. Inset in (C) shows the temporal change of NADH concentration in the presence of different nanotubes.

(D) Photosynthesis of L-glutamate by glutamate dehydrogenase (GDH) with different types of nanotubes.

Adapted from Kim *et al.*[78] with permission from the 2012 John Wiley & Sons Inc.

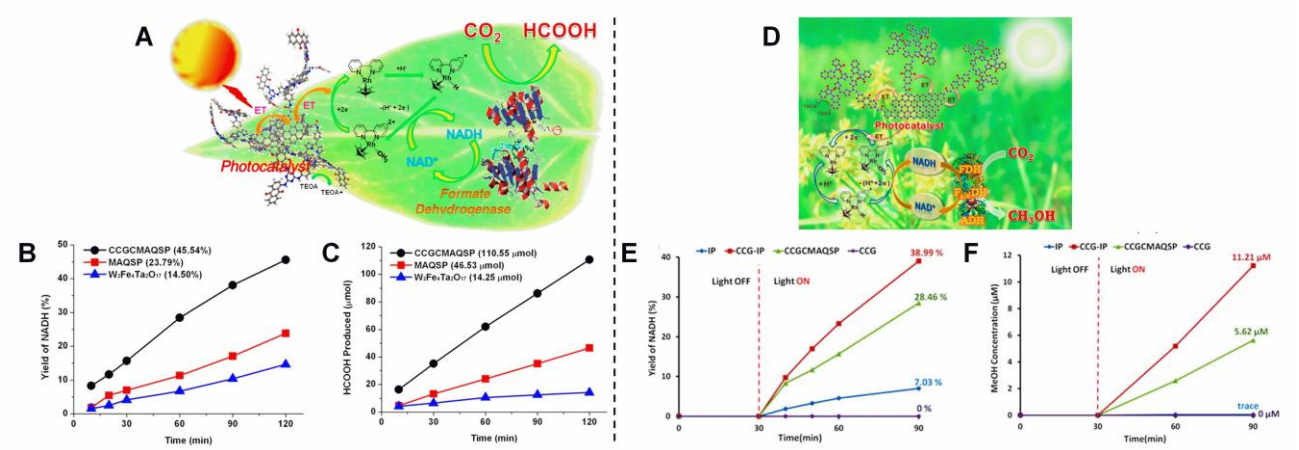

Figure 10. Reaction Schemes of Photocatalytic NADH Regeneration Coupled with Enzymatic Reduction upon CCGCMAQSP-bonded and CCGC-IP-bonded Graphene Nanosheets with Associated Catalytic Performance

(A) CCGCMAQSP-bonded graphene nanosheet photocatalyzed regeneration of NADH and artificial photosynthesis of formic acid from CO_2 under visible light.

(B, C) Photocatalytic activities of CCGCMAQSP and other two photosensitizers in visible-light driven (B) NADH photocatalytic regeneration and (C) artificial photosynthesis of formic acid from CO_2.

Adapted from Yadav *et al.*[79] with permission from the 2012 American Chemical Society.

(D) CCGC-IP-bonded graphene nanosheet photocatalyzed regeneration of NADH and artificial photosynthesis of methanol from CO_2 under visible light.

(E, F) Photocatalytic activities of CCGC-IP and other two photosensitizers in visible-light driven (E) NADH photocatalytic regeneration and (F) artificial photosynthesis of methanol from CO_2.

Adapted from Yadav *et al.*[80] with permission from the 2014 American Chemical Society.

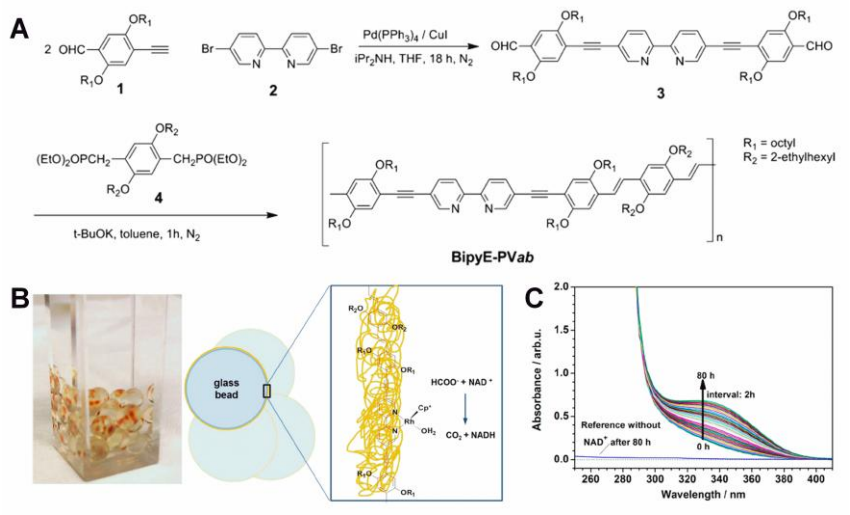

Figure 11. Synthesis, Photocatalytic Application and Performance of the Bipyridine-containing Polymer

(A) Synthesis procedure of the bipyridine-containing polymer (*bipyridine-containing poly-(arylene-ethynylene)-alt-poly(arylene-vinylene) copolymer*).

(B) Experimental setup (left) and scheme of the surface reaction (right) in the chemical reduction of NAD^+ to NADH with formate as hydride donor to the polymer-bound rhodium catalyst reaction center.

(C) UV−vis spectra of the chemical reduction of NAD^+ with formate.

Adapted from Oppelt *et al*.[94] with permission from the 2014 American Chemical Society.

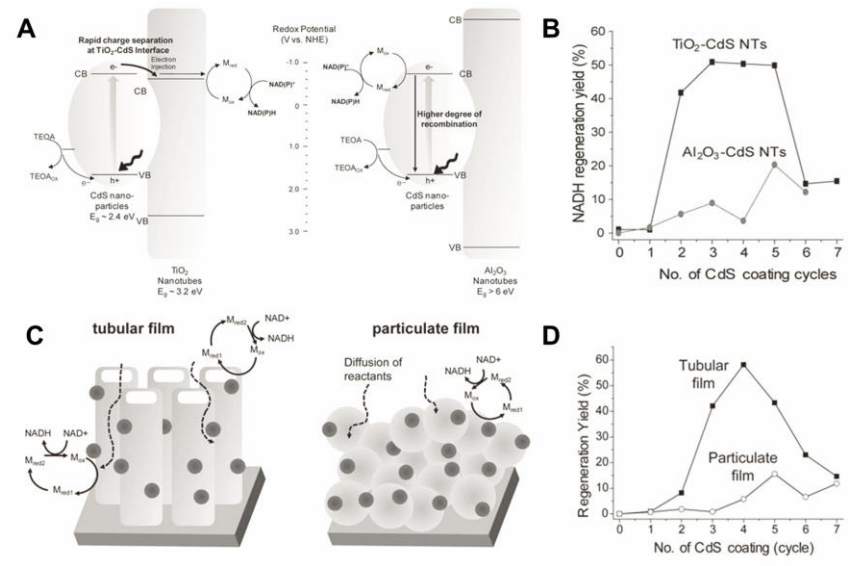

Figure 12. Reaction Mechanism of Photocatalytic NADH Regeneration upon CdS/TiO_2 or CdS-Al_2O_3 Nanotubular Film and the Catalytic Performance

(A) Proposed mechanism for higher efficiency of NADH photocatalytic regeneration by CdS-TiO_2 nanotubular film than CdS-Al_2O_3 nanotubular film.

(B) Comparison between the NADH regeneration efficiencies enabled by CdS-TiO_2 nanotubular film and CdS-Al_2O_3 nanotubular film with different degrees of CdS loading.

(C) Schematic illustration explaining the higher efficiency of NADH photoregeneration obtained with a TiO_2-CdS nanotubular film.

(D) Photoregeneration of NADH using a nano-particulate (open circles) and a nanotubular (filled square) TiO_2-CdS film.

Adapted from Ryu *et al.*[81] with permission from the 2011 John Wiley & Sons Inc.

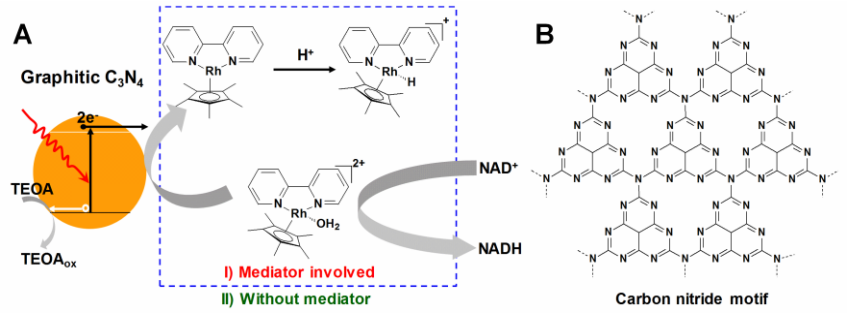

Figure 13. Schematic Illustration of Photocatalytic Regeneration of NADH in the Absence or Presence of Electron Mediator and Structure of g-C_3N_4

(A) Reaction Scheme.

(B) g-C_3N_4 constructed from heptazine building blocks.

Adapted from Liu *et al.*[87] with permission from the 2013 Royal Society of Chemistry.

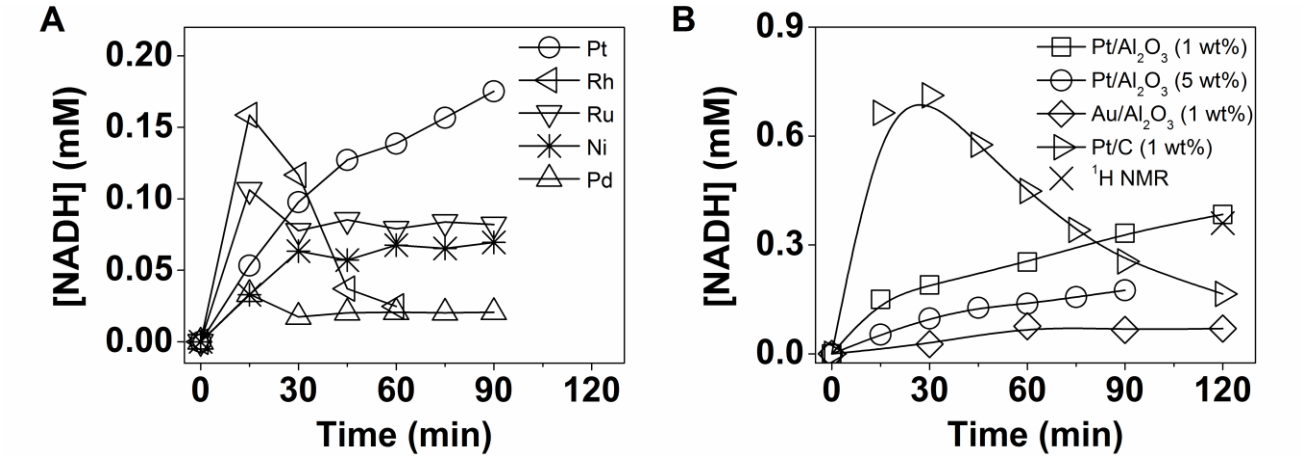

Figure 14. Heterogeneous Catalysts Promoted NADH Regeneration by the Reduction of NAD^+ Using H_2

Variation of NADH concentration as a function of time over (as received) Al_2O_3 supported:

(A) 5 wt% Pt (○), Rh (◁), Ru (▽), Pd (△) and (homemade) 6 wt% Ni (✳).

(B) 1 wt% Pt/Al_2O_3 (□), Pt/C (▷), Au/Al_2O_3 (◇) and 5 wt% Pt/Al_2O_3 (○) with NADH concentration determined by ^1H NMR (×).

Reaction conditions: T = 37 ℃, P = 9 atm, pH = 7, $[NAD^+]_0$ = 1.5 mM and 25 mg catalyst.

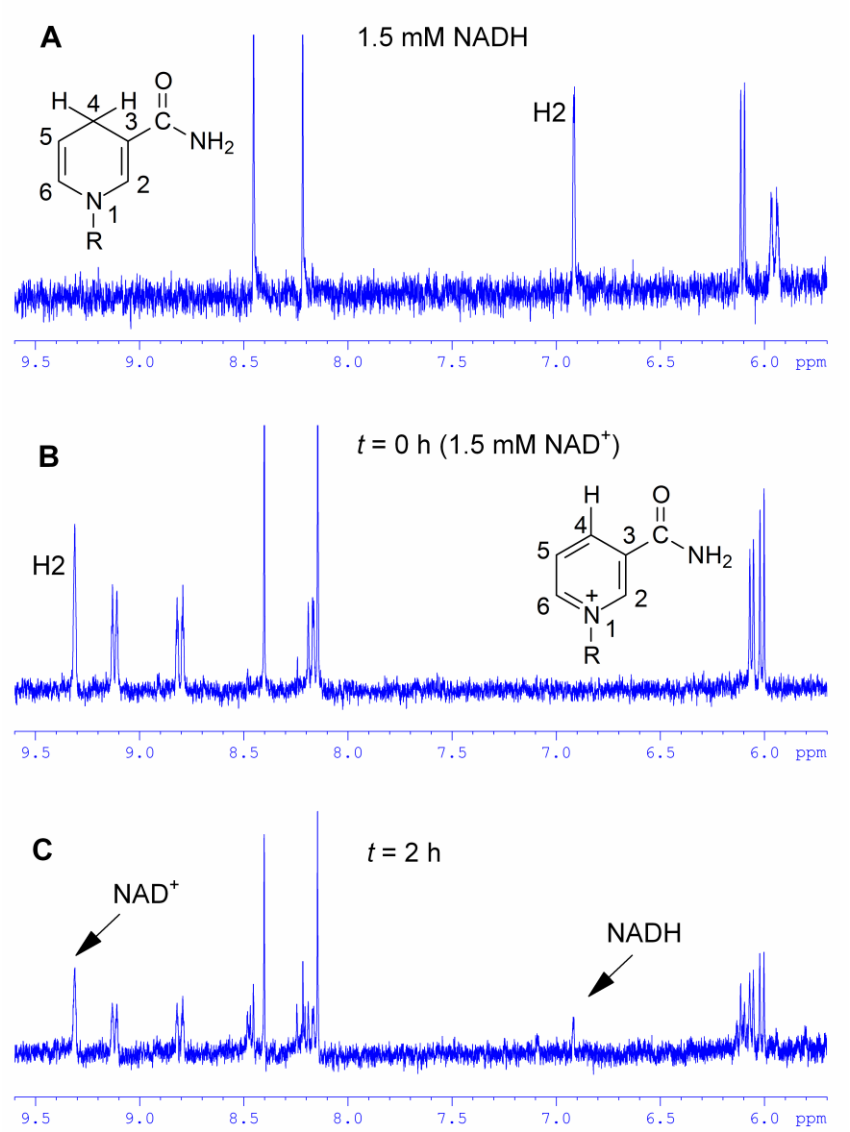

Figure 15. ^{1}H NMR Spectra

(A) 1.5 mM NADH in 100 mM phosphate D_2O buffer (pH = 7.0).

(B) 1.5 mM NAD^+ in 100 mM phosphate D_2O buffer (pH = 7.0).

(C) Reaction product mixture after 2 h (*T* = 37 ℃, pH = 7.0, *P* = 9 atm and 25 mg catalyst, in D_2O buffer).

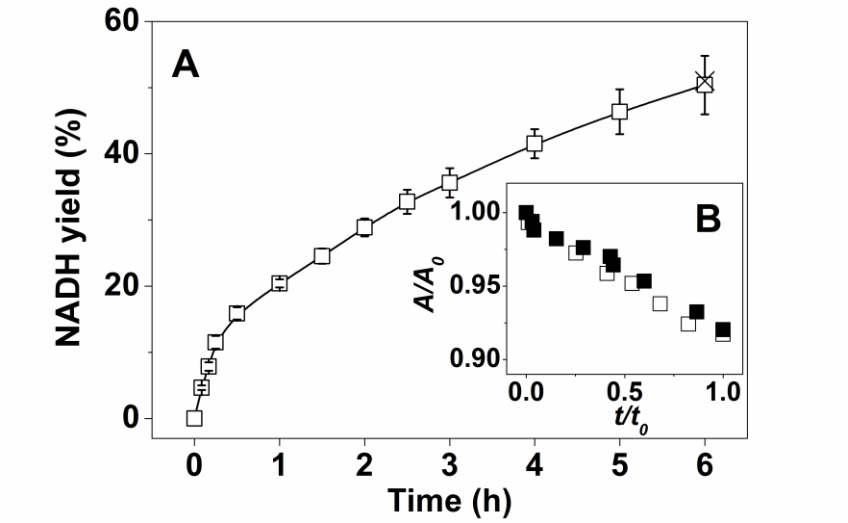

Figure 16. Pt/Al_2O_3 (1 wt%) Catalyzed NAD^+ Reduction for NADH Regeneration

(A) Variation of NADH yield as a function of time (□) with NADH yield determined by ^1H NMR (×).

(B) NADH yield validation using enzymatic assay (EC 1.8.1.4): time dependence of normalized absorbance (A/A_0) of NADH produced experimentally (□) and from a prepared mixture using commercial NADH and NAD^+ (■): A_0 is the absorbance recorded before the enzymatic assay; A is the absorbance recorded after reaction is initiated; t_0 is the total run time of the enzymatic assay; t is the time after initiating the reaction.

Reaction conditions: T = 37 ℃, P = 9 atm, pH = 7, $[NAD^+]_0$ = 1.5 mM and 25 mg catalyst.

Adapted from Wang and Yiu.[12] with permission from the 2016 American Chemical Society.

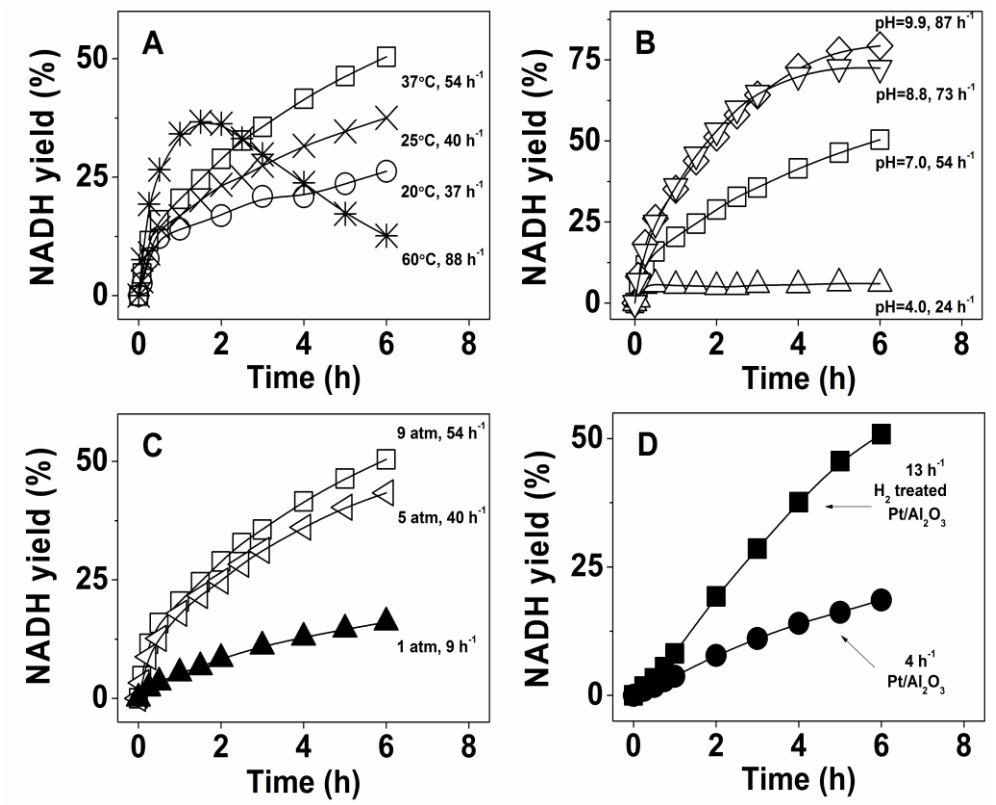

Figure 17. Temporal Variation of NADH Yield and Initial Turnover Frequency (*TOF*, h^{-1}) As A Function of Reaction Parameters in Pt/Al_2O_3 (1 wt%) Catalyzed NAD^+ Reduction for NADH regeneration

(A) Temperature (20 ℃ (○) 25 ℃ (×), 37 ℃ (□) and 60 ℃ (✳) at *P* = 9 atm, pH = 7.0).

(B) pH (4.0 (△), 7.0 (□), 8.8 (▽) and 9.9 (◇) at *T* = 37 ℃, *P* = 9 atm).

(C) Pressure, (1 atm (▲), 5 atm (◁) and 9 atm (□) at *T* = 37 ℃, pH = 7.0).

(D) H_2 treatment (Pt/Al_2O_3 as received (●) and H_2 treated Pt/Al_2O_3 (■) at *T* = 20 ℃, *P* = 1 atm, pH = 8.8).

Other reaction conditions: $[NAD^+]_0$ = 1.5 mM and 25 mg catalyst.

Adapted from Wang and Yiu.[12] with permission from the 2016 American Chemical Society.

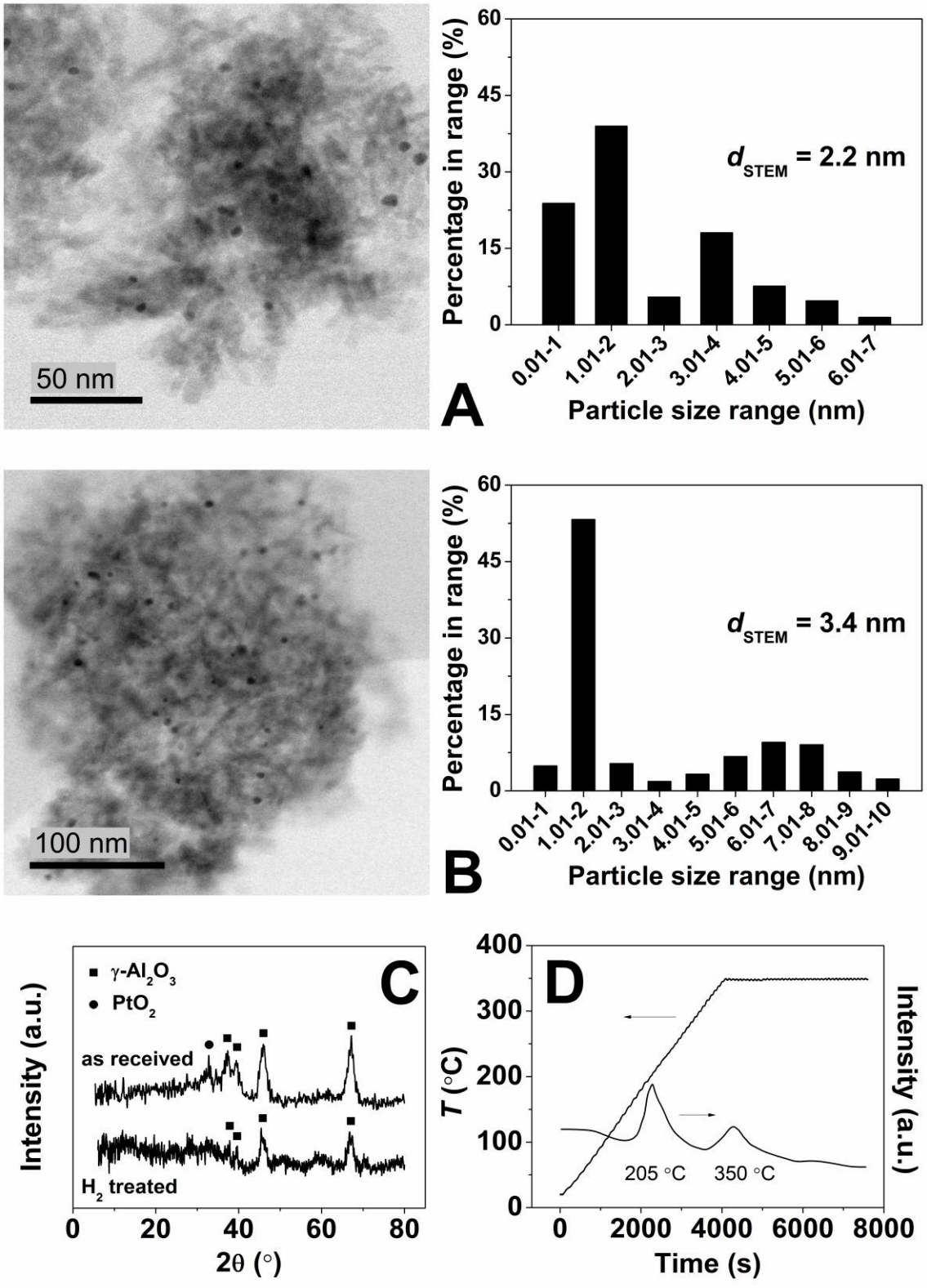

Figure 18. Characterization of Pt/Al_2O_3 (1 wt%)

(A) Representative STEM image and Pt particle size distribution of the as received Pt/Al_2O_3.

(B) Representative STEM image and Pt particle size distribution of the H_2 treated Pt/Al_2O_3.

(C) XRD patterns for the as received and H_2 treated Pt/Al_2O_3.

(D) TPR profile of the as received Pt/Al_2O_3.

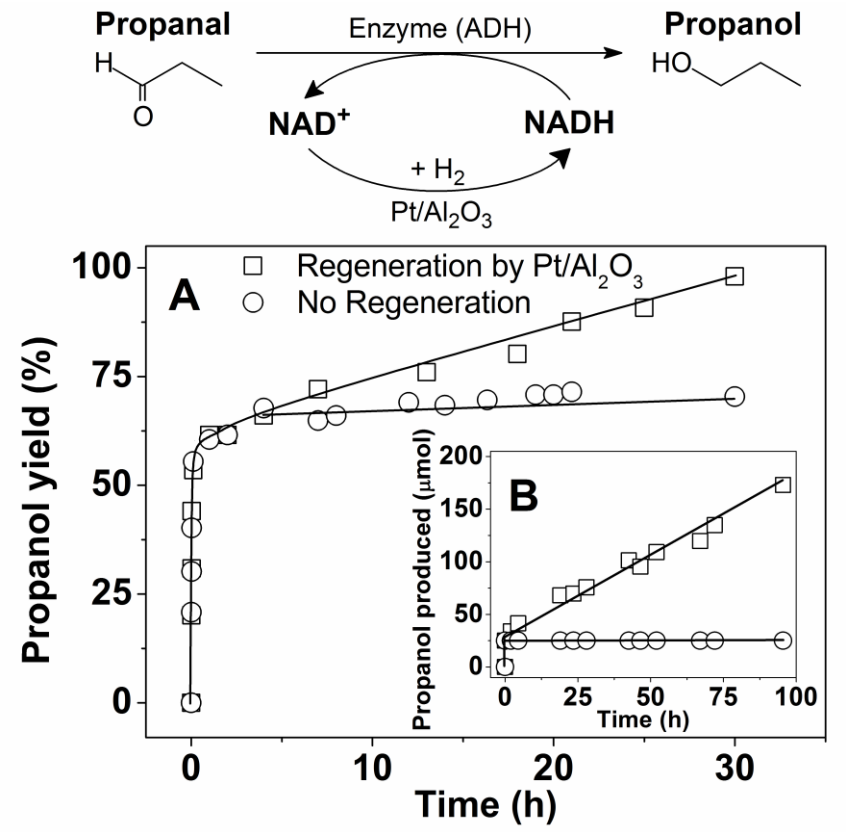

Figure 19. Enzymatic Reduction of Propanal to Propanol Coupled with *In Situ* NADH Regeneration by Pt/Al_2O_3

(A) Temporal propanol yield in batch enzymatic (ADH) reduction of propanal.

(B) Propanol production as a function of time in continuous enzymatic reduction of propanal. Reaction conditions: T = 20 ℃, P = 1 atm (H_2 flow = 30 cm^3 min^{-1}), pH = 8.8 and 25 mg catalyst: (A) $[NADH]_0$ = 7.0 mM and $[propanal]_0$ = 10 mM aand (B) initial NADH = 25 μmol with propanal (2 mM) feed rate = 2.5 cm^3 h^{-1}.

Adapted from Wang and Yiu.[12] with permission from the 2016 American Chemical Society.